Available online at www.sciencedirect.com
ScienceDirect
Colloids and Surfaces B: Biointerfaces 63 (2008) 64–72
COLLOIDS AND SURFACES B
www.elsevier.com/locate/colsurfb

Photografting of 2-methacryloyloxyethyl phosphorylcholine from polydimethylsiloxane: Tunable protein repellency and lubrication property

Tatsuro Goda [a], Ryosuke Matsuno [a], Tomohiro Konno [a], Madoka Takai [a], Kazuhiko Ishihara [a,b,*]

[a] *Department of Materials Engineering, School of Engineering and Center for NanoBio Integration, The University of Tokyo, 7-3-1 Hongo, Bunkyo-ku, Tokyo 113-8656, Japan*
[b] *Department of Bioengineering, School of Engineering and Center for NanoBio Integration, The University of Tokyo, 7-3-1 Hongo, Bunkyo-ku, Tokyo 113-8656, Japan*

Received 13 September 2007; received in revised form 8 November 2007; accepted 11 November 2007
Available online 28 November 2007

Abstract

The phosphorylcholine group functional methacrylate monomer, 2-methacryloyloxyethyl phosphorylcholine (MPC), was graft polymerized from the polydimethylsiloxane (PDMS) substrate using ultraviolet irradiation and using benzophenone as a photoinitiator. The varying monomer concentrations and irradiation times were investigated in order to verify the relationships between graft density and protein resistance under specific biological conditions. The ellipsometry analysis revealed that the layer thickness of the grafted polymer depended on the monomer concentrations after the irradiation for 1 min, however, it stabilized thereafter in all the specified conditions. The curve fitting of the C1*s* spectrum obtained by X-ray photoelectron spectroscopy analysis showed that the amount of grafted polymer increased with an increase in both monomer concentration and irradiation time. Atomic force microscopic images revealed that the terminations among the graft chains became dominant due to magnified chain mobility followed by growth of their length. *In vitro* albumin and fibrinogen adsorption results indicated that the resistance to protein adsorption was easily tuned by the specified conditions due to the controlled graft density. Lubrication was dramatically enhanced by the grafting and it was further promoted by an increase in the graft density in good solvents, indicating that the interactions between the graft chains and the solvents resulted in the lubrication system. These basic findings regarding the grafted PDMS surface are important for versatile applications, including its use as a biomaterial and microfluidic device.

Keywords: Polydimethylsiloxane; Phosphorylcholine; Photografting; Protein adsorption; Lubrication

1. Introduction

Photoinduced graft polymerization has been studied for more than five decades [1–9]. It involves polymerization of acrylic or vinyl monomers from reactive sites on a substrate toward bulk phases. Due to its thermodynamic advantages, the surface-initiated graft polymerization, frequently termed the "grafting from" method, can generate denser brush structures as compared to those generated by polymer grafting to the substrate [10–13]. In addition, Yang and Ranby have demonstrated the photoinduced radical polymerization using benzophenone (BP) as a photoinitiator that favored living polymerization at the low free radical concentrations and the low chain mobility [9]. It is recognized as one of the most useful techniques for the modification and functionalization of polymeric substrates. As a result, this technique has been applied in the fields of bioengineering [14,15] and biomaterials [16–23]. Recently, the photoinduced graft polymerizations from a polydimethylsiloxane (PDMS) substrate with hydrophilic monomers has generated interest as a novel technique capable of controlling wetting behavior or to gain biocompatibility over the native characteristics of PDMS such as low toxicity, good thermal and oxidative stability, low

* Corresponding author at: Department of Materials Engineering, School of Engineering and Center for NanoBio Integration, The University of Tokyo, 7-3-1 Hongo, Bunkyo-ku, Tokyo 113-8656, Japan. Tel.: +81 3 5841 7124; fax: +81 3 5841 8647.
E-mail address: ishihara@mpc.t.u-tokyo.ac.jp (K. Ishihara).

0927-7765/$ – see front matter © 2007 Elsevier B.V. All rights reserved.
doi:10.1016/j.colsurfb.2007.11.014

modulus and cost efficiency [24–27]. In general, non-specific protein adsorptions on polymeric biomaterial interfaces must be prevented from occurring or well be controlled. This is because the adsorption of proteins is the first event that mediates the intercellular reactions with synthetic substrates, or it dramatically decreases the signal to background ratio of microfluidic analytical and enzyme-linked immunosorbent assay (ELISA) systems [28]. However, it is also increasingly important for constructing a surface that exhibits a controlled resistance to proteins, controlled adhesive forces of cells or selected adsorption of biomolecules with regards to tissue engineering and bioengineering [14,15].

In our previous study, a preparation of protein resistant surface on a PDMS substrate was successfully prepared by the photoinduced graft polymerization of 2-methacryloyloxyethyl phosphorylcholine (MPC) [29]. The MPC used was a biomimetic methacrylate that comprises a zwitterionic phosphorylcholine headgroup in its side chain. It was designed according to the cell membrane structure whose surface was covered with a lipid bilayer comprising phosphorylcholine groups. The surface modified with polymers containing MPC forms a membrane analogous structure that mediates mild interactions of biomolecules with synthetic substrates. Several polymeric materials containing MPC units have exhibited strong resistance to protein and they subsequently hinder the following unfavorable biological responses such as thrombus formation, cytotoxic reactions, immunological reactions and inflammatory responses initiated by non-specific protein adsorption [30–40]. The previous study on the photografting of MPC demonstrated that the irradiation time of the ultraviolet (UV) rays determined the amount of poly(MPC) (PMPC) grafted and water wettability on the surface without disturbing the original properties of PDMS [29]. In general, the two-step process that the localization of photoinitiator at the surface and photoinduced polymerization favors the graft polymerization and reduces homo-polymerization in solution [9]. The release of photoinitiator into exposed monomer solution is very limited due to the low solubility of BP in aqueous media, although this technique relies on the simple adsorption of BP onto the substrate. Nevertheless, the scanning of probe microscopic images revealed that the resultant surface formed a hydrogel-like structure rather than the polymer brush. The formation of hydrogel layer was believed to be the crosslink formation, solution polymerization and heat polymerization by elongated exposure of 120 min to UV lamp. So, the graft polymerization induced by UV irradiation in a short period needs to be investigated. In addition, the previous study did not answer the following questions: (1) Is graft density related to protein resistance? (2) Can protein resistance be controlled? (3) When do the termination reactions become dominant? Considering the above questions, the surface-initiated graft polymerization was conducted under specific conditions with regards to the irradiation time and monomer concentration. In order to control the graft density, a two-step irradiation procedure was employed in the experiment. The graft density depends on the activation rate of BP and this in turn, on the irradiation time. Hence, graft density should be controlled by irradiation time. Although this two-step reaction inevitably produces homo-polymers and crosslinked polymers, the effect of the side reactions are neglected during the short duration of UV irradiation. Our future goal for this study is to control the non-specific and specific protein adsorption in order to generate advanced microfluidic devices and artificial organs.

In addition to its antibiofouling property, a significantly low frictional behavior was observed on PMPC-coated and -grafted surfaces under wet conditions [16–21]. The highly hydrated or solvated phosphorylcholine groups present in the PMPC are believed to be responsible for this lubrication property. The hygroscopic and water retentive nature of PMPC facilitates formation of a layer of synovial fluid on the surface of polymeric materials. Hence, the relationship between the amount of grafted PMPC and the friction coefficient was also examined in this study. Interactions of the phosphorylcholine group with various types of solvent molecules also influence the lubrication property due to the conformational changes in PMPC. Friction tests were conducted in water, ethanol and in a mixture of these two solvents in order to examine the effect of their interactions with regard to lubrication.

2. Experimental

2.1. Materials

PDMS (Silpot 184®) and its curing agent were purchased from Toray-Dow Corning Asia Co. Bovine serum albumin and bovine plasma fibrinogen were purchased from Sigma-Aldrich Japan. Dulbecco's phosphate buffered saline was purchased from Immuno-Biological Laboratories (Takasaki, Japan) and used according to the manufacturer's instructions. Unless stated otherwise, all other materials were purchased from commercial sources and used as received. MPC was synthesized according to a previously described method [41] and was recrystallized from acetonitrile.

2.2. Preparation of PDMS substrate

The PDMS network is generally formed by a hydrosilylation reaction between vinyl-terminated oligomeric dimethylsiloxanes and a methylhydrosiloxane using a platinum complex as catalyst. PDMS and the curing agent were mixed well in a ratio of 10:1 by mass. The mixture was evenly spread on a glass plate in the desired shape and degassed under vacuum for 2 h at 25 °C. Then, the curing reaction performed at 60 °C for 6 h at normal atomosphere. Prior to the graft polymerization, the PDMS was cleaned by oxygen plasma (300 W, 100 mL/min flow) for 1 min.

2.3. Graft polymerization of MPC on PDMS substrate

The PDMS was immersed for 1 min in a 30 mL acetone solution containing 1 wt% BP. The membrane was dried *in vacuo* in the dark for 1 h at 25 °C. MPC aqueous solutions were prepared at concentrations of 0.04, 0.10 and 0.25 M in degassed pure water and passed through argon for 10 min to remove the dissolved oxygen. The BP-coated PDMS was set between the glass-plates filled with the MPC solution. The 10-$\mu L/cm^2$ MPC

solution was placed between the PDMS and slide glasses. Photoinduced polymerization was conducted on the PDMS by using a 400 W ultra-high pressure mercury lamp (UVL-400HB, Riko Co, Funabashi, Japan) at wavelength ranging from 312 to 577 nm at distance of 10 cm (9×10^4 lx) for the desired times at 30 °C without using optical filter. After the reaction, the membrane was washed in water and in ethanol for each 15 min and dried for 24 h at room temperature.

2.4. Conversion of BP to semipinacol on PDMS substrate

The total percentage of semipinacol, i.e. the amount of covalently attached BP on PDMS out of physically attached BP, was calculated as follows on the basis of the change in the amount of attached BP: covalently attached BP $(\%) = \{(W_0 - W_1)/W_0\} \times 100$, where W_0 is the amount of detached BP per area without irradiation and W_1 is the amount of detached BP per area after irradiation for the desired time. The amount of physically attached BP was determined by applying 251 nm UV absorption to the ethanol solution. The disc-shaped PDMS (10 mm diameter, 0.3 mm thickness) was immersed in 5.0 mL ethanol, and ultrasonication was performed for 60 min in order to detach the BP from the PDMS membrane.

2.5. Surface characterization

The fluid tapping AFM images in water were analyzed using the NanoScope IIIa (Nihon Veeco, Tokyo, Japan). A fluid cell was used for the measurements. The square pyramidal silicon nitride tips with a height of 2.5–3.5 μm that were mounted on the triangular silicon nitride cantilevers were used with a spring constant of 0.32 N/m. The excitation frequency used was approximately 7–9 kHz. The scan rate was 0.5–1.0 Hz and the imaging size was 1 μm × 1 μm. The root-mean-square (RMS) roughness at 1 μm × 1 μm ($n = 5$) and the area occupied by a single chain were determined using bundled software.

The thickness of the graft layer was determined using an ellipsometer (DVA-36L3, Mizojiri Optical, Tokyo, Japan) with a He–Ne laser (632.8 nm) at an incident angle of 70° under dry conditions at 25 °C. The refractive indices (n_r) of the PDMS and MPC were referenced as 1.63 and 1.49, respectively, and the extinction coefficients (k_e) were 0.00 [42–44] in both cases. Data was collected from nine locations for each sample.

The surface elemental composition was determined using X-ray photoelectron spectroscopy (XPS) (AXIS-His 165, Shimadzu/Kratos, Hadano, Japan) with the magnesium anode non-monochromatic source. All the samples were completely dried *in vacuo* prior to use. High resolution scans for C1*s*, O1*s*, N1*s*, P2*p* and Si2*p* were performed at takeoff angles of 90° and 20°. The C1s signal originated from hydrocarbon was used for adjusting binding energy at 285.0 eV. The curve fitting for each of the components was performed as a Gaussian–Lorentzian sum function. The structure of the polymer repeat unit and knowledge on the chemical shifts obtained from previous literature were used to determine the number, position and area ratio of the component peaks [45]. The atomic concentrations of the elements were determined by their corresponding peak areas.

Advancing and receding contact angles were measured using a dynamic contact angle analyzer (DCA-100W, A & D, Tokyo, Japan) based on the Wilhelmy plate method. The samples were automatically dipped in water at a speed of 80 μm/s to a depth of 15 mm and then withdrawn to the initial position at the same speed. The measurements were repeated five times. The angles were calculated using bundled software.

2.6. Protein adsorption

In vitro single protein adsorption experiments were conducted in a PBS environment. The samples were dipped in 4.5 mg/mL bovine serum albumin ($Mw = 6.7 \times 10^4$) and 0.3 mg/mL bovine plasma fibrinogen ($Mw = 3.4 \times 10^5$), respectively. First, the films were hydrated in PBS for 24 h. Then, the specimens were moved into wells containing a single protein solution and adsorptions were allowed to proceed at 37 °C for 2 h under gentle shaking. Subsequently, each film was gently rinsed in fresh PBS by shaking 50 times without exposure to air. Next, the samples were transferred into wells containing 1 mL PBS solution and 1 wt.% sodium dodecyl sulphate (SDS) and the adsorbed protein was completely desorbed by sonication for 20 min. A protein analysis kit (Micro BCA™ protein assay reagent kit, #23235, Pierce, Rockford, IL, USA) was used to determine the concentration of the detached protein in the SDS solution calculated from the absorbance at 560 nm by using an absorptiometer (Wallac 1420 ARVO sx, PerkinElmer) [46]. This technique is detergent compatible and can quantify various types of dilute protein solutions (0.5–20 μg/mL). The adsorbed amount per unit area was calculated by the amount of detached protein and the surface area of the samples. The mean value at $n = 4$ (±standard deviation) for each condition was obtained.

2.7. Friction coefficient

The surface frictional coefficients of steady (kinetic) states were measured using a tribo-tester (Heidon type32, Shinto Science, Tokyo, Japan). Rectangular sections of the membranes (25 mm × 45 mm) were obtained and were completely doused in the solvents during measurements. The measurements were conducted by sliding the membrane under a load of 1.96 N using a stainless steel ball (10 mm diameter). The scan speed was 10 mm/s, and the scan scale was 20 mm.

3. Results and discussion

3.1. Initiation and termination of the graft polymerization of MPC

The reaction of graft polymerization is illustrated in Fig. 1. Firstly, the physically adsorbed BP onto PDMS was excited by UV irradiation to the triplet state. Then, it extracts a hydrogen atom from an alpha-methyl group of the PDMS to generate a radical being capable of initiating the graft polymerization of MPC. Thus, the sequential graft polymerization was performed.

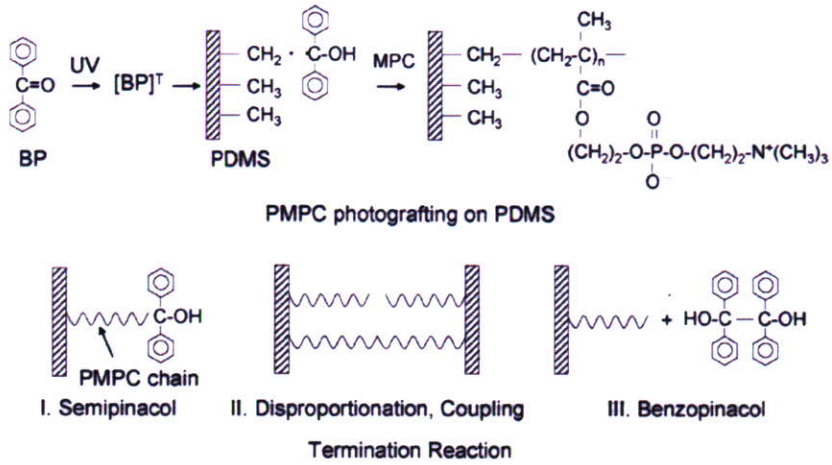

Fig. 1. Schematic description of PMPC grafting from a PDMS substrate using BP as the photoinitiator and the three conceivable termination reactions.

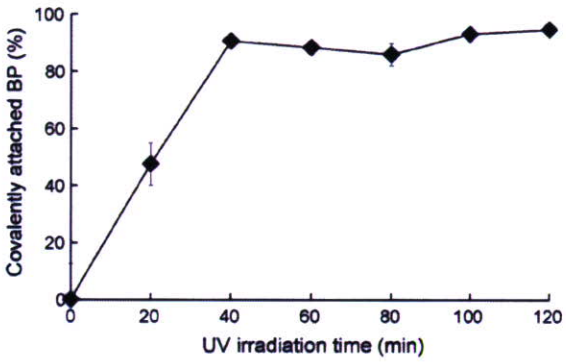

Fig. 2. Percentages of covalently attached BP onto PDMS versus UV irradiation time.

As the activation amount of BP depends on the irradiation period, the graft density should depend on UV irradiation time. The activation rate was quantitatively determined by measuring the absorbance at 251 nm in an ethanol solution after detachment of BP using sonicator for 60 min. Our result was in good agreement with the above mentioned hypothesis. Fig. 2 illustrates the total percentage of semipinacols out of physically absorbed BP onto the PDMS (6.4×10^{-7} mol/cm^2) versus the UV irradiation time. Our data revealed that 90% of BP was proportionally excited during the initial 40 min of irradiation, and no further covalent attachment of BP occurred thereafter.

The difference between free radical polymerization and living radical polymerization is in terms of their terminations. Most semipinacol radicals in the end chains deactivate by terminations. There are three conceivable termination reactions with regard to the semipinacol radical as illustrated in Fig. 1. Among these terminations, disproportionation, coupling and production of benzopinacol prevent further growth of the graft chains. Semipinacol group is only capable of reinitiating the graft polymerization by UV irradiation. However, the UV source used in the study was in the region of UVA (315–400 nm) and it does not activate semipinacol for polymerization. Disproportion and coupling reaction that prohibit further polymerization increases with the length of the graft chain. Therefore, the graft polymerization is stopped by the inactive terminations and nonuniformity of the graft chain increased with an increase in the reaction time. The atomic force microscope (AFM) images directly revealed the discordant state of grafted polymer chains. Fig. 3(a)–(c) display the tapping mode AFM images of the PMPC-grafted PDMS surfaces with varying irradiation times at an area of 1 μm^2 in water. Since the surface of the original PDMS was nearly flat, the fine polymer chains were observed at the PMPC-grafted surface with a photo irradiation of 1 min. By

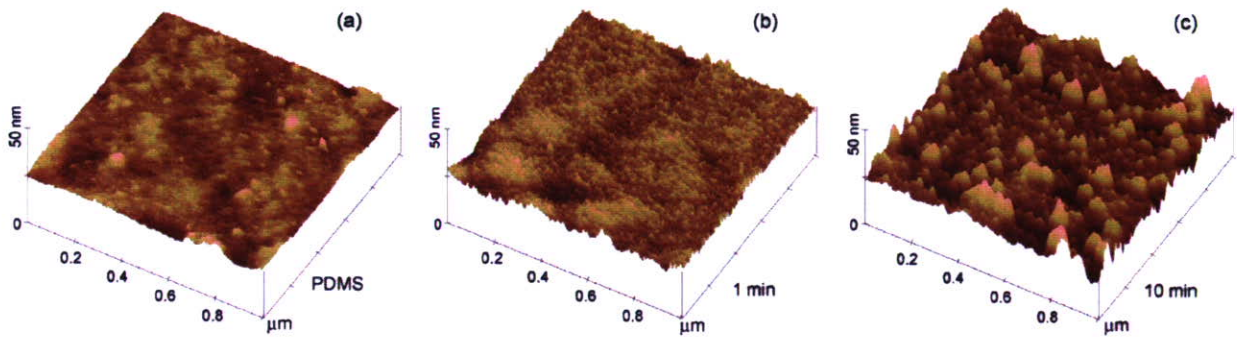

Fig. 3. Tapping mode AFM topographical images in water. The original PDMS surface (a), PMPC-grafted surface prepared in 0.25 M of monomer under UV irradiation for 1 min (b) and PMPC-grafted surface prepared in 0.25 M of monomer under UV irradiation 10 min (c).

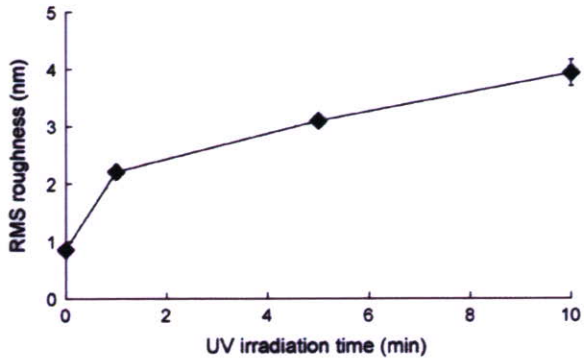

Fig. 4. Relationships between the surface RMS roughness of a 1 μm^2 area in water ($n = 5$) and UV irradiation time.

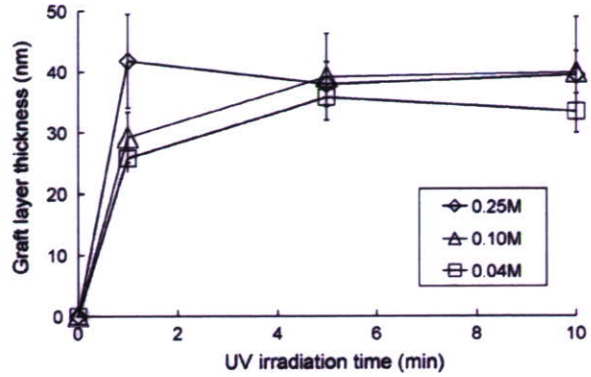

Fig. 5. PMPC-grafted layer thickness under dry condition obtained from ellipsometry versus UV irradiation time with varying monomer concentrations (◇: 0.25 M, △: 0.10 M, □: 0.04 M).

using a top-view AFM image, the average circular area occupied by a single graft chain was measured to be approximately 50–100 nm^2 ($r = 5$ nm). Hence, the chain density was measured as approximately 0.01–0.02 chain/nm^2. Despite the bulkiness of the phosphorylcholine group in the PMPC, the graft density was relatively low, and under such conditions, the graft chains formed mushroomed structures rather than brush structures. On the other hand, the generation of the PMPC chain aggregates was observed on increasing the irradiation time to 10 min. The average area increased to approximately 350 nm^2 ($r = 10$ nm). As for certain giant aggregates, it exceeded 2000 nm^2 ($r > 25$ nm). Since it was unlikely that the aggregate comprised a single chain, it probably comprised several chains due to the terminations caused by the increased chain density and mobility or by crosslinks among the PMPC chains. In addition, Fig. 4 shows the average of the RMS roughness at a specific 1 μm^2 area in water on the grafted surfaces with varying UV irradiation times. The RMS roughness increased with an increase in the UV irradiation time due to the coexistence of continuously growing and immediately terminating chains. This result sufficiently explains the nonuniformity caused by the inactivation of the semipinacol due to the termination reactions.

3.2. Characterization, thickness and density of the PMPC graft chain

Fig. 5 shows the relationships between the thickness of the grafted PMPC layer and UV irradiation time at various monomer concentrations under dry conditions. The layer thickness depended on the irradiation time for the initial 5 min at lower monomer concentrations and subsequently stabilized, whereas it did not depend on the irradiation time at a higher monomer concentration of 0.25 M. Further clarification is required to explain the inconsistency between this observation and our previous report with regard to the relationship between the thickness of the grafted PMPC layer and UV irradiation time. However, the incomplete deoxygenation of the monomer solution often prohibits graft polymerization. In the present study, better elimination of oxygen from the fed monomer solution may have facilitated a successful increase in the graft layer thickness within the short duration of UV irradiation. The limitation in the increase of the layer thickness to 30–40 nm was due to the termination reactions that were facilitated by the increased mobility of terminal semipinacol owing to the increased length of the graft chains. The reaction rate generally increases with an increase in the monomer concentration. Hence, the chain

Table 1
Elemental compositions on the PMPC-grafted PDMS prepared surface

Monomer concentration (M)	UV irradiation time (min)	Elemental composition (atom%)*									
		Takeoff angle 90°					Takeoff angle 20°				
		C	O	N	P	Si	C	O	N	P	Si
0.04	1	33.7	42.6	0.8	0.6	22.3	46.1	31.3	0.4	0.5	21.7
0.04	5	41.9	37.5	1.4	1.4	17.8	48.9	29.1	0.6	0.9	20.5
0.04	10	37.0	40.3	1.0	0.9	20.8	44.0	33.2	0.6	0.8	21.4
0.10	1	35.2	41.9	0.8	0.8	21.3	45.7	31.9	0.3	0.6	21.5
0.10	5	46.4	34.5	2.0	2.0	15.1	47.1	31.7	0.8	1.0	19.4
0.10	10	43.1	37.0	1.6	1.3	17.0	51.0	28.4	1.2	0.9	18.5
0.25	1	33.1	44.3	1.2	0.8	20.6	43.8	33.3	1.0	0.8	21.1
0.25	5	48.0	33.1	2.5	1.0	15.4	51.3	27.7	2.0	1.0	18.0
0.25	10	43.5	36.9	1.9	1.7	16.0	51.2	29.7	0.7	1.1	17.3
PDMS		46.1	30.8	0.0	0.0	23.1	46.6	28.4	0.0	0.0	25.0

*Elemental compositions were calculated using the XPS analysis performed at a photoelectron takeoff angle of 90° and 20°.

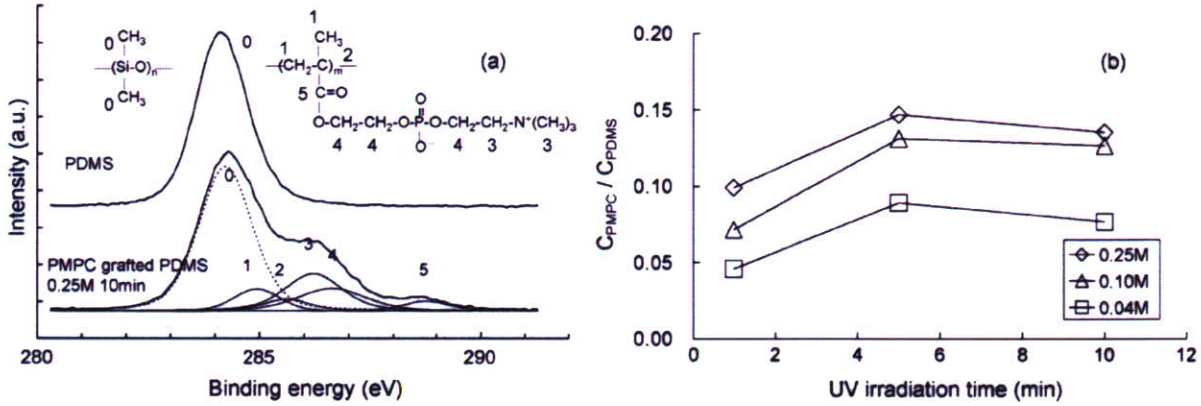

Fig. 6. Peak fittings of the C1*s* XPS spectra for the PMPC-grafted PDMS and the original PDMS surfaces at a photoelectron takeoff angle of 90° (a). Compositional ratios of PMPC to PDMS calculated by the C1*s* peak area versus UV irradiation time with varying monomer concentrations (◇: 0.25 M, △: 0.10 M, □: 0.04 M) (b).

ceases to grow after 1 min due to the terminations followed by a rapid growth of the graft chains at a higher monomer concentration.

XPS provides us quantitative and qualitative information regarding the elements that existed in depth with ≤10 nm on a polymeric surface [47]. Table 1 shows the elemental compositions on the PMPC-grafted PDMS at takeoff angles of 90° and 20° determined by peak areas of C1*s*, O1*s*, N1*s*, P2*p* and Si2*p*. Existence of N and P elements were only confirmed on the grafted surface. The higher compositions of N and P were due to an increase in the amount of graft polymer, whereas these compositions measured at a takeoff angle of 90° were higher than those measured at 20°. It can be explained by the experimental conditions of ultrahigh vacuum. Hydrophilic graft chains of PMPC would be buried and hydrophobic PDMS appear under a high vacuum environment [47].

Core level chemical shifts provide a reasonable degree of information regarding its organic structure. Fig. 6(a) displays the high resolution C1*s* XPS spectra of the original PDMS and the PMPC-grafted PDMS at a photoelectron takeoff angle of 90°. The C1*s* spectrum for the grafted surface was smoothly fitted into six peaks. The 284.3 eV peak was associated with the methyl group in PDMS and the other carbon peaks at 285.0, 285.7, 286.3, 286.7 and 288.8 eV were associated with each functional moiety in PMPC. The C1*s* peaks of the PMPC were associated with each carbon as shown in Fig. 6(a), and the ratios of the peak areas were almost proportional to the number of carbon atoms in the MPC. Fig. 6(b) illustrates the compositional ratio of PMPC to PDMS. This ratio was calculated by addition of the areas for each polymer and the number of carbon elements. Unlike with the ellipsometric result, the composition of PMPC was increased with an increase in monomer concentration, indicating that the amount of grafted polymer depended on the monomer concentration. Considering that the graft layer thickness reached plateau at the specific monomer concentrations and irradiation times, the increased amount of grafted polymer can be accepted to be the result of the increased graft density. The amount of grafted polymer also increased with irradiation time for the first 5 min. However, it stabilized afterward at any monomer concentrations. The results indicate that the termination reaction occurred within 10 min of UV irradiation. Further, initiation of graft polymerization from the substrate was prevented due to the insufficient room for new PMPC chains although a substantial amount of unreacted BP remained on the PDMS surface.

In general, contact angle measurement is the most convenient method to assess changes in the wetting characteristics of polymeric biomaterials. Fig. 7 displays the dynamic contact angle changes for PMPC-grafted surfaces irradiated at monomer concentrations of 0.25, 0.10, and 0.04 M. The surface rapidly adapted a hydrophilic nature in the presence of the PMPC graft chain and its hydrophilicity increased with an increase in irradiation time. A greater reduction in advancing contact angle (from 120° to 60°) was observed during the initial 10 min of irradiation at monomer concentration of 0.25 and 0.10 M due to the increased graft density. However, the receding contact angles dramatically decreased for the initial 1 min under higher monomer concentrations and stabilized thereafter. The receding contact angles decreased with an increase in monomer concentration, indicating that the receding contact angles depended on the graft density. This wetting behavior was produced by high water absorptivity of phosphorylcholine group in the PMPC, and Kitano et al. hypothesized that the presence of thickly hydrated water generated by the phosphorylcholine group exhibit protein

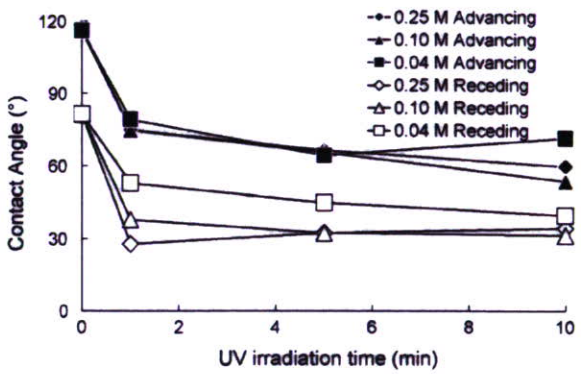

Fig. 7. Advancing (black marks) and receding (white marks) water contact angles for the PMPC-grafted PDMS prepared in varying monomer concentrations (◇: 0.25 M, △: 0.10 M, □: 0.04 M) versus UV irradiation time.

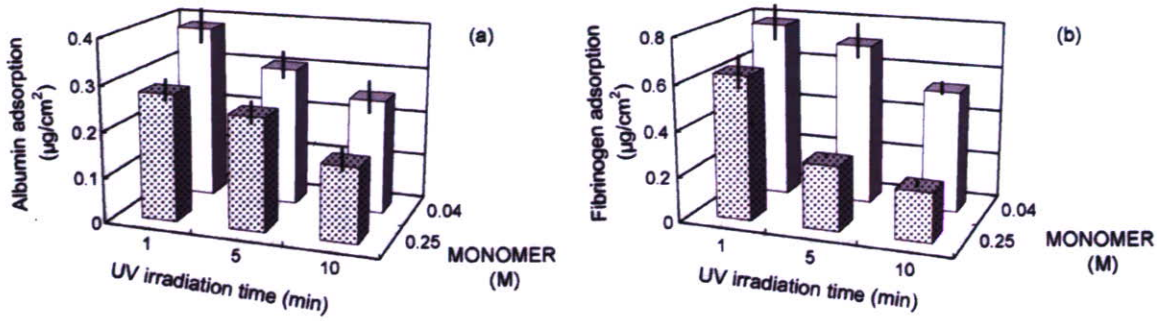

Fig. 8. Amount of *in vitro* albumin (a) and fibrinogen (b) adsorbed onto the PMPC-grafted PDMS surfaces prepared by different monomer concentration and irradiation time.

resistance [48–50]. The hysteresis, i.e. the difference between the advancing and receding angles, is indicative of the mobility of the graft chain, and it decreased with an increase in irradiation time. Hence, the increased chain density and terminations followed by UV irradiation resulted in a loss of the graft chain mobility.

3.3. Resistance to protein adsorption

The amount of albumin and fibrinogen present on the surface prepared under different conditions is displayed in Fig. 8(a) and (b), respectively. The results revealed that both albumin and fibrinogen adsorptions decreased with an increase in UV irradiation time and the monomer concentration. The amount of albumin and fibrinogen adsorptions on the original PDMS was $0.41 \pm 0.06\ \mu g/cm^2$ and $0.80 \pm 0.06\ \mu g/cm^2$, respectively. The reductions in the amount of adsorbed protein were a result of the increase in graft density of the PMPC on the PDMS. This is because the ellipsometric result indicated that the graft chain length was constant under the specified experimental conditions but the XPS results revealed that the amount of graft chain length increased with an increase in irradiation time and monomer concentration. This observation is consistent with that of the previous reports by Iwata et al. [42] and Feng et al. [43,44] that refer to the increased density and length of the PMPC graft chain prepared by atom transfer radical polymerization (ATRP) resisted protein adsorption *in vitro*. The amount of albumin adsorbed did not decrease further at the irradiation duration of more than 10 min at 0.25 M (data not shown). A large amount of albumin and fibrinogen was adsorbed onto the surfaces that was prepared using brief UV irradiation duration and dilute monomer concentration due to the low density of the PMPC chain. The PDMS surface could not be completely covered with the PMPC graft chains on this surface. These results indicate that the sufficient resistance to protein adsorption occurs only on a surface that has high graft density of PMPC. In other words, the tendency of protein adsorption can be easily tuned by altering irradiation time. This technique would be important in the field of bioengineering to perform processes such as the surface modification in microfluidic device channels to control cell adhesion or attachment on a substrate. Kitano et al. have reported that zwitterionic groups had a very minor effect onto the structure of the hydrogen-bonding network of water molecules that produce the resistance to non-specific protein adsorption [48–50]. Recent computer simulations using molecular dynamics have supported their results. Tamai et al. have demonstrated that the average hydrogen-bond number for water in the vicinity of hydrophilic groups of polymers is smaller than that observed in pure water, and the hydrogen-bond number is slightly lower than that in pure water in the hydrophobic region. The water–water hydrogen bond is especially stabilized in the presence of alkyl chains due to hydrophobic hydration [51,52].

3.4. Lubrication property in solvents

Extraordinary lubricity on the PMPC-modified surfaces under wet condition has also been studied. Our previous data suggested that the highly hydrated PMPC layer dramatically decreased the friction coefficient [18]. The relationship between the frictional coefficient and number of graft chains was also examined in the study. The data also suggested that the solvation around the PMPC chains affected its lubrication property. In order to obtain more information regarding the frictional behavior of the PMPC, the relationship between the kinetic friction coefficient and irradiation time was investigated in water, ethanol and a mixture of the two solvents (70% ethanol by volume). Fig. 9 displays the single logarithmic plots of the kinetic friction coefficient and irradiation time under dry and solvent conditions. The result demonstrated that the friction coefficients decreased with an increase in irradiation time in all the solvents.

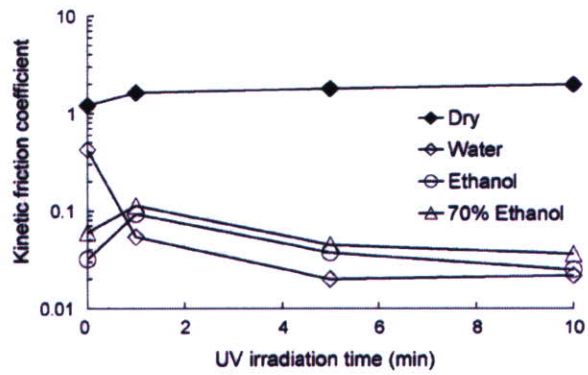

Fig. 9. Kinetic friction coefficients in various solvents versus UV irradiation time (0.25 M of MPC).

This indicates that the increased graft density enhanced surface lubrication. This is clearly due to the increased lubrication effect generated by the good solvation property. The frictional coefficient on the PMPC-grafted surface was lowest in water, followed by pure ethanol and 70% ethanol. This phenomenon can be explained by the hydrophobic hydration of solvents around phosphorylcholine [53,54]. It is known that the PMPC chain solvated in water and ethanol change to globule state in 70% ethanol by desolvation. This is because hydrophobic hydration of the water molecules around phosphorylcholine group forming clathrate via hydrogen bonds each other is disrupted by the large amount of ethanol molecules. The polymer desolvation may result in the loss of fluid lubrication system. However, further quantitative and qualitative investigation is required with regard to solvation and the conformation of the graft chains in order to have a better understanding of the lubrication system. Muller et al., for example, reported that the nano-frictional characteristic of a poly(ethylene glycol)-grafted surface was associated with the actual amount of adsorbed solvent per graft chain [55].

4. Conclusions

This study described the initiation, termination and surface properties of photoinduced graft polymerization of MPC on a PDMS substrate using BP as a photoinitiator. Increased UV irradiation time and monomer concentration increased the density of the grafted polymer. However, the chain length remained constant after initial irradiation due to termination of the semipinacols in the end chain. Resistance to protein adsorption, water wettability and lubrication characteristics were tunable with the graft density. These observations are important with regard to surface modifications of polymeric biomaterials with controlled protein adsorption and cell adhesion.

Acknowledgements

We thank Professor T. Hanawa at Tokyo Medical and Dental University for the measurement of ellipsometry. One of the authors (T.G.) thanks the partial support from JSPS Research Fellowship for young scientists.

References

[1] G. Oster, O. Shibata, J. Polym. Sci. 26 (1957) 233.
[2] A.N. Wright, Nature 215 (1967) 953.
[3] R.P. Seiber, H.L.J. Needles, J. Appl. Polym. Sci. 19 (1975) 2187.
[4] Y. Ogiwara, M. Kanda, M. Takumi, H. Kubota, J. Polym. Sci., Polym. Lett. Ed. 19 (1981) 457.
[5] Z. Yao, B. Ranby, J. Appl. Polym. Sci. 41 (1990) 1469.
[6] E. Uchida, Y. Uyama, Y. Ikada, J. Appl. Polym. Sci. 47 (1993) 417.
[7] M. Ulbricht, H.H. Schwarz, J. Membr. Sci. 136 (1997) 25.
[8] H. Ma, R.H. Davis, C.N. Bowman, Macromolecules 33 (2000) 331.
[9] W. Yang, B. Ranby, Macromolecules 29 (1996) 3308.
[10] B. Zhao, W.J. Brittain, Prog. Polym. Sci. 25 (2000) 677.
[11] K. Kato, E. Uchida, E.T. Kang, Y. Uyama, Y. Ikada, Prog. Polym. Sci. 28 (2003) 209.
[12] A. Bhattacharya, B.N. Misra, Prog. Polym. Sci. 29 (2004) 767.
[13] M. Ulbricht, Polymer 47 (2006) 2217.
[14] W. Senaratne, L. Andruzzi, C.K. Ober, Biomacromolecules 6 (2005) 2427.
[15] K.L. Christmanab, V.D. Enriquez-Riosa, H.D. Maynard, Soft Matter 2 (2006) 928.
[16] T. Goda, T. Konno, M. Takai, K. Ishihara, Colloid Surf. B-Biointerfaces 54 (2007) 67.
[17] S.P. Ho, N. Nakabayashi, Y. Iwasaki, T. Boland, M. LaBerge, Biomaterials 24 (2003) 5121.
[18] T. Moro, Y. Takatori, K. Ishihara, T. Konno, Y. Takigawa, T. Matushita, U. Chang, K. Nakamura, H. Kawaguchi, Nat. Mater. 3 (2004) 829.
[19] M. Kyomoto, T. Moro, T. Konno, H. Takadama, N. Yamawaki, H. Kawaguchi, Y. Takatori, K. Nakamura, K. Ishihara, J. Biomed. Mater. Res. Part A 82 (2007) 10.
[20] M. Kyomoto, Y. Iwasaki, T. Moro, T. Konno, F. Miyaji, H. Kawaguchi, Y. Takatori, K. Nakamura, K. Ishihara, Biomaterials 28 (2007) 3121.
[21] Y. Iwasaki, M. Takamiya, R. Iwata, S. Yusa, K. Akiyoshi, Colloid Surf. B-Biointerfaces 57 (2007) 226.
[22] Y. Iwasaki, S. Sawada, N. Nakabayashi, G. Khang, H.B. Lee, K. Ishihara, Biomaterials 20 (1999) 2185.
[23] K. Ishihara, Y. Iwasaki, S. Ebihara, Y. Shindo, N. Nakabayashi, Colloid Surf. B-Biointerfaces 18 (2000) 325.
[24] S. Hu, X. Ren, M. Bachman, C.E. Sims, G.P. Li, N.L. Allbritton, Anal. Chem. 76 (2004) 1865.
[25] Y. Wang, M. Bachman, C.E. Sims, G.P. Li, N.L. Allbritton, Langmuir 22 (2006) 2719.
[26] Q. Pu, O. Oyesanya, B. Thompson, S. Liu, J.C. Alvarez, Langmuir 23 (2007) 1577.
[27] M. Ebara, J.M. Hoffman, A.S. Hoffman, P.S. Stayton, Lab. Chip 6 (2006) 843.
[28] E. Eteshola, D. Leckband, Sens. Actuator B-Chem. 72 (2001) 129.
[29] T. Goda, T. Konno, M. Takai, K. Ishihara, Biomaterials 27 (2006) 5151.
[30] K. Ishihara, R. Aragaki, T. Ueda, A. Watenabe, N. Nakabayashi, J. Biomed. Mater. Res. 24 (1990) 1069.
[31] K. Ishihara, N.P. Ziats, B.P. Tierney, N. Nakabayashi, J.M. Anderson, J. Biomed. Mater. Res. 25 (1991) 1397.
[32] K. Ishihara, K. Oshida, T. Ueda, Y. Endo, A. Watanabe, N. Nakabayashi, J. Biomed. Mater. Res. 26 (1992) 1543.
[33] T. Ueda, K. Ishihara, N. Nakabayashi, J. Biomed. Mater. Res. 29 (1995) 381.
[34] J.D. Patel, Y. Iwasaki, K. Ishihara, J.M. Anderson, J. Biomed. Mater. Res. Part A 73 (2005) 359.
[35] K. Ishihara, E. Ishikawa, A. Watanabe, Y. Iwasaki, K. Kurita, N. Nakabayashi, J. Biomater. Sci. Polm. Edn. 10 (1999) 1047.
[36] S. Sawada, S. Sakaki, Y. Iwasaki, N. Nakabayashi, K. Ishihara, J. Biomed. Mater. Res. Part A 64 (2003) 411.
[37] S. Sawada, Y. Iwasaki, N. Nakabayashi, K. Ishihara, J. Biomed. Mater. Res. Part A 79 (2006) 476.
[38] J.K.W. Lam, Y. Ma, S.P. Armes, T. Baldwin, S.J. Stolnik, J. Control. Release 100 (2004) 293.
[39] K. Ishihara, H. Nomura, T. Mihara, K. Kurita, Y. Iwasaki, N. Nakabayashi, J. Biomed. Mater. Res. 39 (1998) 323.
[40] Y. Matsuda, M. Kobayashi, M. Annaka, K. Ishihara, A. Takahara, Chem. Lett. 35 (2006) 1310.
[41] K. Ishihara, T. Ueda, N. Nakabayashi, Polym. J. 22 (1990) 355.
[42] R. Iwata, P. Suk-In, V.P. Hoven, A. Takahara, K. Akiyoshi, Y. Iwasaki, Biomacromolecules 5 (2004) 2308.
[43] W. Feng, S. Zhu, K. Ishihara, J.L. Brash, Langmuir 21 (2005) 5980.
[44] W. Feng, S. Zhu, K. Ishihara, J.L. Brash, Biointerphases 1 (2006) 50.
[45] G. Beamson, D. Briggs, High Resolution XPS of Organic Polymers, John Wiley & Sons, England, 1992, Chapter 15.
[46] P.K. Smith, R.I. Krohn, G.T. Hermanson, A.K. Mallia, F.H. Gartner, M.D. Provenzano, E.K. Fujimoto, N.M. Goeke, B.J. Olson, D.C. Klenk, Anal. Biochem. 150 (1985) 6.
[47] L. Ruiz, J.G. Hilborn, D. Leonard, H.J. Mathieu, Biomaterials 19 (1998) 987.
[48] H. Kitano, K. Sudo, K. Ichikawa, M. Ide, K. Ishihara, J. Phys. Chem. B 104 (2000) 11425.
[49] H. Kitano, M. Imai, T. Mori, M. Gemmei-Ide, Y. Yokoyama, K. Ishihara, Langmuir 19 (2003) 10260.

[50] H. Kitano, S. Tada, T. Mori, K. Takaha, M. Gemmei-Ide, M. Tanaka, M. Fukuda, Y. Yokoyama, Langmuir 21 (2005) 11932.
[51] Y. Tamai, H. Tanaka, K. Nakanishi, Macromolecules 29 (1996) 6750.
[52] Y. Tamai, H. Tanaka, K. Nakanishi, Macromolecules 29 (1996) 6761.
[53] Y. Kiritoshi, K. Ishihara, J. Biomater. Sci. Polym. Edn. 13 (2002) 213.
[54] Y. Kiritoshi, K. Ishihara, Sci. Technol. Adv. Mater. 4 (2003) 93.
[55] M.T. Muller, X. Yan, S. Lee, S.S. Perry, N.D. Spencer, Macromolecules 38 (2005) 3861.

Available online at www.sciencedirect.com
ScienceDirect
Colloids and Surfaces B: Biointerfaces 62 (2008) 288–298
COLLOIDS AND SURFACES B
www.elsevier.com/locate/colsurfb

Covalent immobilization of antibody fragments on well-defined polymer brushes via site-directed method

Ryoko Iwata [a], Rina Satoh [a,b], Yasuhiko Iwasaki [c,*], Kazunari Akiyoshi [a]

[a] *Institute of Biomaterials and Bioengineering, Tokyo Medical and Dental University, 2-3-10 Kanda-surugadai, Chiyoda-ku, Tokyo 101-0062, Japan*
[b] *Department of Materials and Applied Chemistry, College of Science and Technology, Nihon University, 1-8-14 Kanda-surugadai, Chiyoda-ku, Tokyo 101-8308, Japan*
[c] *Faculty of Chemistry, Materials and Bioengineering, Kansai University, 3-3-35 Yamate, Suita, Osaka 564-8680, Japan*

Received 24 August 2007; received in revised form 12 October 2007; accepted 28 October 2007
Available online 4 November 2007

Abstract

Well-defined polymer brushes and block copolymer brushes consisting of 2-methacryloyloxyethyl phosphorylcholine (MPC) and glycidyl methacrylate (GMA) were prepared by surface-initiated atom transfer radical polymerization (ATRP). The polymer brushes were used for the immobilization of antibody fragments in a defined orientation. Pyridyl disulfide moieties were introduced to the polymer brushes via a reaction of epoxy groups in GMA units. Fab' fragments were then immobilized onto these surfaces via a thiol-disulfide interchange reaction and the reactivity of antibodies with antigens was investigated. Antigen/antibody binding on the polymer brushes was more preferable than that on epoxysilane films as a control surface. Furthermore, the activity of the antibodies immobilized on the block copolymer brushes having biocompatible PMPC was greater than that on other surfaces that did not have PMPC in their structures.

Keywords: Surface modification; Polymer brush; ATRP; Phosphorylcholine polymer; Protein immobilization

1. Introduction

There has been great interest in the development of protein biochips because they would be powerful tools for proteomic and diagnostic investigation in obtaining information about protein functions and interactions, and for screening complex protein samples [1,2]. Protein immobilization is a key technology for the successful development of a protein microarray. Strategies for immobilizing proteins on substrates have been studied but considerable development is still required. Amine-, aldehyde-, and epoxide-derivatized glass slides are often used as protein microarray platforms [3]. On these surfaces, proteins are immobilized via a reaction with the amine and carboxyl groups of amino acid residues such as lysine and glutamic acid. However, since these amino acids are usually abundant in proteins, the attachment may occur simultaneously through the many residues that enhance heterogeneity in the population of immobilized proteins [1]. The multipoint attachment also causes structural deformation of the proteins resulting in a partial or total loss of activity [4]. Furthermore, the random orientation of the immobilized proteins decreases the accessibility of the active site. To immobilize proteins in a defined orientation according to site is therefore very important for maintaining the biological activities of proteins. Peluso et al. performed oriented immobilization of antibodies by a specific reaction between biotin and streptavidin using a site-specifically biotinylated antibody [5]. They compared the activity of full-sized antibodies and Fab' fragments immobilized in both a random and oriented state. The increased analyte binding capacity of the surfaces with oriented capture agents was consistently observed over surfaces with randomly oriented capture agents, with improvements up to 10 times greater. In addition, it was demonstrated that Fab' fragments retained 90% of normal activity on average when specifically oriented. Chen and co-workers controlled the orientation of antibodies by changing the surface charge [6,7]. They also utilized the charge distributions of the antibodies. On positively charged surfaces, IgG 1 type antibodies oriented with the antigen-binding domain directed to the liquid phase showing higher reactivity with antigens compared to that of antibodies immobilized on negatively charged surfaces.

* Corresponding author. Tel.: +81 6 6368 0090; fax: +81 6 6368 0090.
E-mail address: yasu.bmt@ipcku.kansai-u.ac.jp (Y. Iwasaki).

0927-7765/$ – see front matter © 2007 Elsevier B.V. All rights reserved.
doi:10.1016/j.colsurfb.2007.10.018

In addition to oriented immobilization of proteins, suppressing nonspecific interactions with biomolecules is crucial for developing highly sensitive protein biochips. Nagasaki et al. performed the co-immobilization of both antibody and PEG on magnetic bead surfaces and showed that the nonspecific adsorption of proteins from cell lysates could easily be reduced [8]. Furthermore, a 20-fold higher S/N ratio was achieved with the antibody/PEG co-immobilized surface compared to a surface treated with bovine serum albumin, a conventional blocking reagent.

Surface modification at the molecular level is then required to control the function of the biomolecules on the surface. In recent years, living radical polymerization has been used for surface-initiated polymerization and well-defined polymer brushes were successfully produced [9–12]. This method is called the "grafting from" system and can be used to prepare dense polymer brushes as compared with the adsorption of functionalized polymers to solid/liquid interfaces, which is called the "grafting to" system due to steric hindrance of the polymers [11]. Atom transfer radical polymerization (ATRP) is one of the methods of living radical polymerization and is studied widely because a wide range of monomers can be used in the process.

In contrast, we have been studying 2-methacryloyloxyethyl phosphorylcholine (MPC) polymers synthesized as biomimetics in biomembrane structures [13–16]. The MPC polymers (PMPC) exhibit a property that resists nonspecific interaction with plasma proteins and cells showing excellent biocompatibility [17,18]. In addition, it has been confirmed that no activation and inflammatory response of cells in contact with PMPC are induced [19,20]. To control the surface structures of PMPC on a submolecular scale for investigating the effect on biofouling, we have prepared PMPC brushes by ATRP. On well-defined PMPC brushes, protein adsorption was effectively reduced. Furthermore, protein and cell manipulations were performed well when the thickness of the polymer brushes was just above 5 nm [21]. Preparation of PMPC brushes by ATRP has been independently and mostly reported by Feng et al. [22,23]. They prepared PMPC brushes with various graft densities from 0.06 to 0.39 chains/nm^2 and chain lengths from 5 to 200 MPC units, and characterized their effect on protein adsorption [23]. Dramatic reductions in fibrinogen adsorption were observed on the surfaces with high graft densities and high PMPC chain lengths. From these experiments, the excellent properties of PMPC brushes to considerably reduce protein adsorption and cell adhesion were demonstrated.

In previous work, we performed block copolymerization of glycidyl methacrylate (GMA) from PMPC brushes for engineering biomaterial surfaces [24]. Polymer brushes have been applied for biological analysis and their effectiveness in accumulating proteins and oligonucleotides was demonstrated [25,26]. Immobilization of probe molecules in high density in a defined area is also required for the highly sensitive detection of analytes on protein biochips. It is especially crucial for the fabrication of micro- and nanoscale devices. It was also shown that the block architecture ensured good accessibility of the immobilized probe [26]. There are few reports on the immobilization of proteins by polymer brushes having nonfouling properties [27] in defined orientation [28]. Further, to the best of our knowledge, investigation of the control of polymer brush structure and its influence on biological reactions considering the oriented immobilization of proteins, the accumulation of probes, and the suppression of nonspecific adsorption has not yet been reported. Here, we report the oriented immobilization of antibody fragments on well-defined polymer brushes consisting of GMA and biocompatible MPC.

2. Materials and methods

2.1. Materials

Silicon wafers (100 orientation, P/B doped) were purchased from Yamanaka Semiconductor Co., Ltd., Tokyo, Japan. MPC was synthesized by previously reported methods [29]. GMA and ethyl-2-bromoisobutyrate were purchased from Tokyo Chemical Industry Co., Ltd., Tokyo, Japan, and Sigma-Aldrich, Japan, respectively, and purified by distillation before use. 3-(2-Bromoisobutyryl)propyl dimethylchlorosilane (BDCS) was synthesized as previously described [30,31]. Purified water (reverse osmosis) was further purified on a Millipore Milli-Q system that involves reverse osmosis, ion exchange, and filtration steps (18.2 MΩ cm). Goat anti-mouse IgG F(ab')$_2$ fragment and goat anti-mouse IgG fluorescein isothiocyanate (FITC) conjugate F(ab')$_2$ fragment were purchased from Sigma-Aldrich, Japan. Mouse anti-rat IgG FITC conjugate was obtained from Zymed Laboratories, Inc., California, USA, and donkey anti-rabbit IgG rhodamine conjugate was purchased from Cosmo Bio Co., Ltd., Tokyo, Japan. Other chemicals were used as received without further purification.

2.2. BDCS monolayers on silicon wafer

Silicon wafers were cut into 1.2 cm × 1.2 cm pieces, cleaned before use by ultrasound in toluene for 5 min, and rinsed with toluene, absolute acetone, and absolute ethanol. After being dried in an argon gas stream, the wafers were washed by O_2 plasma for 30 min and placed in a clean oven at 120 °C for 2 h. Silanization was immediately performed after treatment of the plates.

The BDCS monolayer on the silicon wafer was prepared by the method previously reported [21,31]. Briefly, cleaned silicon wafers were held in a custom-designed holder and placed in a dry flask to which 30 mL of dry toluene, triethylamine (21 μL, 0.15 mmol), and BDCS (33 μL, 0.15 mmol) were added under an argon gas atmosphere. The flask was allowed to stand for 72 h. The wafers were then removed from the solution, rinsed with toluene, absolute acetone, and absolute ethanol, and dried in an argon gas stream.

2.3. Preparation of well-defined polymer brushes

Methanol was used as a solvent for the atom transfer radical polymerization of MPC. The solvent was purged with argon at an elevated temperature, which was higher than the boiling point of methanol. After boiling for 5 min, the solvent was cooled to room temperature under argon to eliminate any oxygen before the polymerization. Copper(I) bromide (CuBr) (29 mg,

0.20 mmol) and 2,2′-dipyridyl (bpy) (63 mg, 0.41 mmol) were dissolved in 9 mL of methanol, and ethyl-2-bromoisobutyrate (EBIB) (30 μL, 0.20 mmol) was added as a sacrificial initiator. After being stirred for 30 min under an argon gas atmosphere, the BDCS-immobilized silicon wafers were then submerged into the flask. MPC (12.0 g, 41 mmol) was separately dissolved in 21 mL of methanol and the solution was purged with argon for at least 30 min before use. The MPC solution was then added to the flask and polymerization occurred at room temperature with stirring under an argon gas atmosphere. After polymerization for 30 min and 1 h, the silicon wafers were removed from the polymerization mixture and immediately submerged into the solution for GMA polymerization.

GMA was polymerized from PMPC brushes immediately after the MPC polymerization. A mixed solvent of 7 parts methyl–ethyl–ketone (MEK) and 3 parts ethanol was used as the solvent. CuBr (8.6 mg, 0.060 mmol), bpy (19 mg, 0.12 mmol), and EBIB (9 μL, 0.060 mmol) were dissolved in 21 mL of MEK and 9 mL of ethanol in a new flask with stirring under an argon gas atmosphere during the polymerization of MPC. The silicon wafers with the PMPC brushes were submerged into this solution. GMA (1.6 mL, 0.012 mol) purged with argon for 30 min was added and polymerization occurred at room temperature with stirring under an argon gas atmosphere. The silicon wafers were periodically removed from the polymerization mixture and rinsed with THF, acetone, and ethanol. Subsequently, the wafers were extracted with a Soxhlet apparatus in THF overnight and dried in an argon gas stream. They were then washed by ultrasound in water, rinsed with ethanol, and dried in an argon gas stream.

A PMPC brush and a PGMA brush were prepared using the same method as described above. After polymerization, the PMPC brush was washed by extraction with a Soxhlet apparatus in methanol and subsequent ultrasound in water. The PGMA brush was washed using the Soxhlet apparatus in THF and sonication in water.

The number-average molecular weight of free MPC polymer in solution was measured with a Tosoh GPC system with a refractive index detector and size-exclusion columns, Shodex SB-804 HQ and SB-806M HQ, with a poly(ethylene glycol) (Tosoh standard sample) standard in distilled water containing 10 mM LiBr. For measurement of the number-average molecular weight of free GMA polymer, KF-803 (Shodex) was used with the Tosoh GPC system. Calibration was performed using a poly(styrene) (Tosoh standard sample) standard and THF was used as the eluent. The structures of the polymers were determined by ^{1}H NMR (α-500, JEOL, Tokyo, Japan).

2.4. Preparation of epoxysilane films on silicon wafer

Epoxysilane films were prepared according to the method previously described [32]. Briefly, silicon wafers were cut and cleaned as described above. The cleaned silicon wafers were held in a custom-designed holder and placed in a dry flask to which 29.7 mL of dry toluene and (3-glycidoxypropyl) trimethoxysilane (Gelest, Inc.) (0.3 mL, 1.4 mmol) were added under an argon gas atmosphere. The flask was allowed to stand for 24 h. The wafers were then removed from the solution, rinsed with toluene, absolute acetone, and absolute ethanol. After subsequent cleaning by ultrasound in absolute ethanol and rinsing with ethanol, the wafers were dried in an argon gas stream.

2.5. Introduction of pyridyl disulfide moieties

Pyridyl disulfide moieties were introduced to the polymer brushes via a reaction of epoxy groups in GMA units. The silicon wafers on which the polymer brushes were prepared were submerged into dithiothreitol (DTT) solution (3 mM DTT, 0.1 M potassium bicarbonate pH 8.5, 0.5 mM EDTA) and allowed to react at room temperature for 15 h with stirring. The wafers were then rinsed with 0.1 M potassium bicarbonate pH 8.5, deionized water, 0.2 M sodium acetate pH 5.0, and deionized water. After being dried with an argon gas stream, the wafers were soaked in a solution of 2,2-dithiodipyridine (2PDS) and 2-thiopyridone (2TP) (34 mM 2PDS, 8 mM 2TP, 50 mM sodium bicarbonate, 45% ethanol) and allowed to react at room temperature for 1.5 h. The wafers were rinsed with 50% ethanol and dried in vacuo.

2.6. Surface analysis

The dynamic contact angles for the sample plates were recorded by use of a probe fluid, deionized water (18.2 MΩ), Gilmont syringes, and a First Ten Angstroms FTÅ125 goniometer. The advancing (θ_A) and receding (θ_R) contact angles were measured with addition to and withdrawal from the drop, respectively.

The thickness of the polymer brush was measured on an auto ellipsometer (DVA-36L3, The Optronics Co., Ltd., Tokyo, Japan) operating with a 632.8 nm He–Ne laser at a 70° incident angle.

X-ray photoelectron spectroscopy (XPS) was performed using a magnesium anode non-monochromatic source (Kratos-Shimadzu, Kanagawa, Japan). Survey scans spectra of C_{1s}, O_{1s}, N_{1s}, P_{2p}, Br_{3d}, and S_{2p} were obtained. Data were collected at take off angles of 15° and 90°.

2.7. Immobilization of Fab' fragments on activated polymer brushes

The $F(ab')_2$ fragments were split into Fab' fragments with 2 mM 2-mercaptoethylamine in 0.1 M sodium phosphate, 5 mM EDTA, pH 6.0 for 1 h at 37 °C. After reaction, excess 2-mercaptoethylamine was removed by running the sample through a column (NAP-25, Amersham) with 0.1 M sodium phosphate, 5 mM EDTA, pH 6.0, as the eluent. The prepared sample was analyzed using 5%–20% SDS-polyacrylamide gel electrophoresis (SDS-PAGE) (samples were diluted with nonreducing protein loading buffer). A ~50 kDa band corresponding to the Fab' fragment [33] was observed. There were few contaminants corresponding to the sizes of the free light chains and the cleaved heavy chains. This antibody fragment solution was used for immobilization to the surfaces.

To determine the area in contacted with the antibody solution, we used silicone rubber and acrylic plates with holes. The silicone rubber was washed by ultrasound in acetone and ethanol before use. The acrylic plates were also cleaned by ultrasound in ethanol. The diameters of the holes were 7.5 mm. The silicon wafers were first covered with silicone rubber, and then put between two acrylic plates, one of which had a hole. They were then fixed in place with clips. A 50 μL solution of 2.6 mg/mL Fab' fragments was added and placed in contact with each surface. Reaction occurred at room temperature for 21 h under humid conditions. The wafers were rinsed with 0.1 M sodium phosphate, 5 mM EDTA, pH 6.0, by changing the contacting solution several times. They were subsequently used for the antigen reaction or the investigation of the nonspecific reaction of antibody fragment-immobilized surfaces. For surface analysis by XPS, the silicone rubber and the acrylic plates were removed from the wafers. Then, the wafers were rinsed again with buffer and deionized water, and dried. To compare the amount of immobilized antibody, we used FITC-labeled Fab' fragments prepared by the reduction of FITC-labeled $F(ab')_2$ fragments as described above. The FITC-labeled Fab' fragments were immobilized on polymer brushes by the same method used for the Fab' fragments. After the reaction and washing with buffer, the silicone rubber and the acrylic plates were removed from the wafers. The wafers were rinsed again with buffer and deionized water, and dried. The fluorescence intensity was then analyzed using a plate reader ($ARVO_{TM}$SXFL, PerkinElmer Japan, Kanagawa, Japan).

2.8. Reaction of immobilized Fab' fragments with antigens

The activity of the immobilized Fab' fragments was investigated. The Fab' fragments were immobilized on polymer brushes as described above. After being rinsed with 0.1 M sodium phosphate, 5 mM EDTA, pH 6.0, the wafers were subsequently washed with phosphate-buffered saline solution (PBS). Then, 50 μL of 1 wt/vol% bovine serum albumin (BSA, Sigma Chemical Co., St. Louis, MO) in PBS was placed in contact with the Fab' fragment-immobilized polymer brushes for 1 h at room temperature to inhibit nonspecific adsorption with the following antigen. FITC-labeled mouse IgG was used as the antigen and diluted 50 times with 1 wt/vol% BSA solution in PBS. Sixty microliters of antigen solution (15 μg/mL) was applied to the wafers and reacted for 1 h at room temperature under humid conditions. After being rinsed with PBS, the silicone rubber and acrylic plates were removed from the wafers. The wafers were rinsed again with PBS and deionized water, and dried. The surfaces were observed with a fluorescent microscope (IX70, OLYMPUS, Tokyo, Japan) and the fluorescence intensity was analyzed.

2.9. Investigation of nonspecific adsorption on Fab' fragment-immobilized surfaces

After the immobilization of the Fab' fragments and washing with 0.1 M sodium phosphate, 5 mM EDTA, pH 6.0 and subsequently with PBS, 60 μL of rhodamine-labeled IgG, which is not the antigen of the Fab' fragments immobilized on the surfaces, was applied. The rhodamine-labeled IgG was diluted with PBS and adjusted to 15 μg/mL before use. IgG solution was placed in contact with each surface for 1 h under humid conditions at room temperature. After being rinsed with PBS, the silicone rubber and the acrylic plates were removed. The samples were rinsed again with PBS and deionized water. After being dried in an argon gas stream, the surfaces were observed with a fluorescent microscope and the fluorescence intensity was analyzed.

3. Results and discussion

3.1. Preparation of well-defined polymer brushes

The block copolymer brushes consisting of PMPC and poly(GMA) (PGMA) were prepared on silicon wafers by surface-initiated ATRP (Scheme 1). First, MPC was polymerized from a BDCS monolayer and GMA was then polymerized from the PMPC brushes immediately after the MPC polymerization.

The polymerization of MPC was performed by the same basic method previously described [21]. We used methanol as the solvent instead of a mixture of water and methanol because we have found that the polymer radical concentration was more constant in methanol than in a mixture of water and methanol (data not shown). We obtained about 7–8 nm thick PMPC brushes with a theoretical molecular weight of 15,000–19,000 for 30 min or 1 h of polymerization time (Table 1). In previous work, we have clarified that serum protein adsorption and fibroblast adhesion could be effectively reduced on PMPC brushes when the brush thickness was above about 5 nm [21]. Thus, we chose PMPC brushes with a brush thickness of about 7–8 nm, which is above 5 nm, and used them for the block copolymerization with GMA.

Fig. 1 shows the kinetics of ATRP of GMA from the end of PMPC. The semilogarithmic plot of monomer concentration vs. time was linear up to 71% conversion. The linearity of the first-order plot of the monomer concentration suggested that the polymer radical concentration remained constant and that polymerization could be controlled on a polymerization time scale. GMA could be polymerized from PMPC brushes and the thickness of PGMA was increased with an increase in polymerization time, as described previously [24]. Block copolymer brushes with a PGMA layer thickness of 4.3 and 7.7 nm, and theoretical

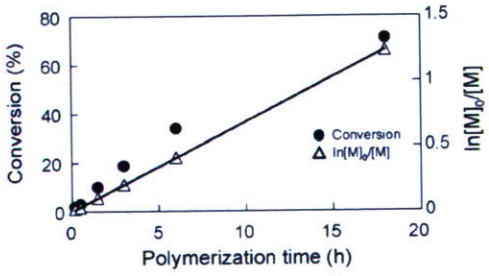

Fig. 1. Kinetics of ATRP of GMA in the block copolymerization evaluated by the analysis of free PGMA in the solution.

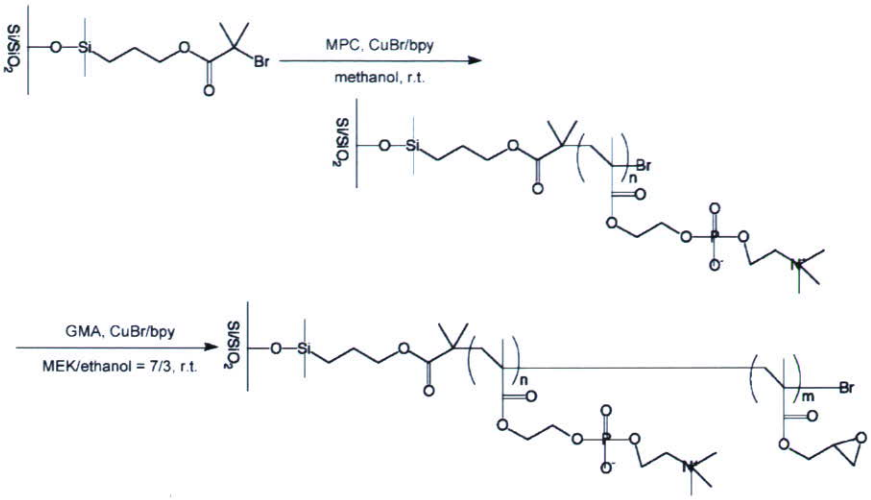

Scheme 1. Synthetic route of block copolymer brushes on silicon wafer by ATRP.

molecular weights of 10,100 and 18,100 were obtained for polymerization times of 6 and 18 h, respectively. The formation of block copolymer brushes confirmed the living character of this polymerization and showed that at least a considerable fraction of the chain ends was still active for initiation of further film growth.

Because the molecular weight of free polymers produced in solution is assumed to be the same as that of polymer chains on the surface [34], we analyzed free polymers by GPC. The M_n obtained by polystyrene calibration increased with an increase in the polymerization time, but there was some deviation from the theoretical value (data not shown). Thus, we used theoretical M_n in the following discussions. The graft density σ (chains/nm^2) of each polymer brush was calculated according to the following equation:

$$\sigma = \frac{h\rho N_A}{M_n} \quad (1)$$

where h is the layer thickness of each polymer layer determined by ellipsometry, ρ is the density of the dry polymer layer (1.30 g/cm^3 for PMPC, 1.0 g/cm^3 for PGMA), N_A is Avogadro's number, and M_n is the number-average molecular weight of the graft polymers (theoretical value). It is reported that the bulkiness of the monomer unit has a steric effect on the behavior of graft polymerization [35] resulting in the lower graft density of the polymer brush consisting of a large-sized monomer than that consisting of a small-sized monomer. This behavior was also observed in this study. A PGMA brush showed a higher graft density than did a PMPC brush consisting of a large-sized monomer compared with a GMA monomer (Table 1). The graft density of the PGMA brush layer in the block copolymer brush was lower than was that of the PGMA brush, which was directly prepared from the BDCS monolayer without the PMPC brush layer. In the block copolymer brush, the graft density of the PGMA unit is regulated by that of the PMPC brush. The lower graft density of the PGMA unit in the block copolymer brush is thus reasonable. This result demonstrates that GMA was indeed polymerized from the ends of the PMPC brushes. We prepared PGMA brushes for comparison with block copolymer brushes in the following experiments. Since PGMA brushes were more densely polymerized than the PGMA layer in the block copolymer brushes, the thickness of the PGMA brushes was higher than that of the PGMA layer in the block copolymer brushes for the same polymerization time. We prepared PGMA brushes having

Table 1
Characteristics of each polymer brush prepared by ATRP[a]

Abbreviation	Polymer thickness (nm)[b]		Graft density[b,c] (chains/nm^2)	Water contact angle (°)[b]	
	PMPC	PGMA		θ_A	θ_R
PMPC18.7K[d]	8.1 ± 1.2	–	0.35 ± 0.0	9.9 ± 2.7	0.0 ± 0.0
PGMA11.0K	–	8.2 ± 0.9	0.43 ± 0.1	71.2 ± 1.9	39.8 ± 4.3
PMPC14.9K-*b*-PGMA10.1K	7.0 ± 0.4	4.3 ± 0.7	0.26 ± 0.05[e]	49.8 ± 11.6	0.0 ± 0.0
PMPC17.5K-*b*-PGMA18.1K	7.9 ± 0.6	7.7 ± 0.7	0.26 ± 0.04[e]	54.5 ± 7.6	0.0 ± 0.0

[a] ATRP conditions: [MPC]/[EBIB]/[CuBr]/[bpy] = 200:1:1:2, [MPC] = 1.0 M for ATRP of MPC; [GMA]/[EBIB]/[CuBr]/[bpy] = 200:1:1:2, [GMA] = 0.4 M for ATRP of GMA.

[b] Mean ± S.D., $n \geq 4$.

[c] Calculated according to Eq. (1) using theoretical M_n.

[d] Theoretical M_n of polymer chain is 18,700 g/mol; theoretical M_n was determined by conversion × targeted DP (200) × MW of monomer (MPC; 295.3 g/mol, GMA; 142.15 g/mol).

[e] Graft density of PGMA brush layer in the block copolymer brush.

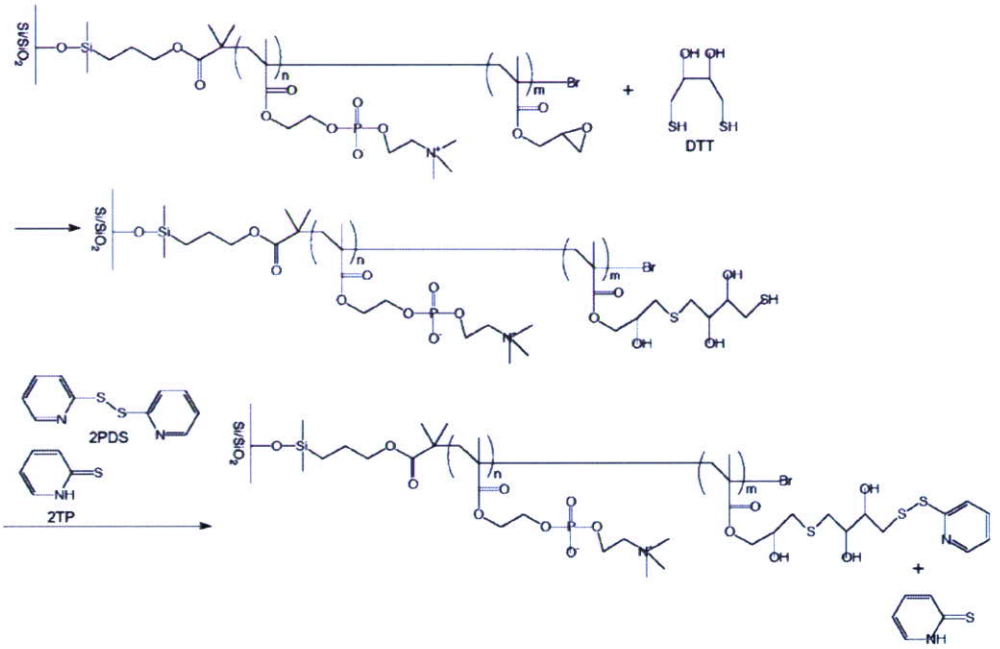

Scheme 2. Synthetic route of the introduction of pyridyl disulfide moieties onto polymer brushes.

a thickness similar to the PGMA unit in the block copolymer brushes. 8.2 nm thick PGMA brushes with a theoretical molecular weight of 11,000 were obtained for a polymerization time of 6 h.

The PMPC brushes showed an extremely low water contact angle because of the hydrophilic nature of PMPC. This value increased after the copolymerization with GMA but it was still lower than that of the PGMA brushes, especially in the receding contact angle. This result implies that the surface property of a block copolymer brush reflected the properties of both PMPC and PGMA. To understand the condition and the conformation of block copolymer brushes precisely, more detailed experiments are needed such as responses to solvents.

Table 1 summarizes the characteristics of each polymer brush prepared. We used these polymer brushes in the following experiments.

3.2. Introduction of pyridyl disulfide moieties

Pyridyl disulfide has been used for covalent immobilization of proteins on supports [36–38] and conjugation of biomolecules [39,40] by a thiol-disulfide interchange reaction. This reaction proceeds under mild conditions and specifically occurs between thiol-disulfide bonds. Since the occurrence of exposed thiols in proteins is usually very low, this method can be used for site-directed immobilization or conjugation of proteins. A Fab' fragment is an antibody fragment that has a thiol group in the opposite side of the antigen-binding domain. Therefore, when we use thiol groups for immobilization, we can immobilize the Fab' fragments in an ordered orientation on substrates without affecting the antigen-binding domain [5]. We introduced pyridyl disulfide moieties onto the polymer brushes to immobilize the Fab' fragments in an ordered orientation. The introduction of pyridyl disulfide moieties was performed according to the method previously described (Scheme 2) [38,41]. Grazú et al. used two reaction steps, the thiolation of epoxy groups with DTT and the activation of thiolated supports with 2-PDS. In the first reaction, they succeeded in controlling the degree of substitution of the epoxy groups by changing the concentration of DTT. They achieved 6.7% and 12.5% conversion when the molar ratio of DTT to epoxy group was 1.8:1 and 3.7:1, respectively, and the reaction time was 1 h at room temperature. In this study, we reacted excess DTT with polymer brushes because the molar ratio of DTT to epoxy group is about 1800:1. Furthermore, the reaction lasted for 15 h. This concentration of DTT and the reaction time seems to be sufficient to substitute a considerable amount of epoxy groups in the polymer brushes. We used 2TP in addition to 2PDS in the second reaction to effectively introduce pyridyl disulfide moieties. 2TP can split the nonreactive disulfide bond formed between two adjacent thiols in the polymer brushes by forming a reactive thiopyridyl group and a free thiol, which is immediately converted to another thiopyridyl group by reaction with 2PDS [41].

After the reaction with 2PDS and 2TP, the introduction of pyridyl disulfide moieties was confirmed by XPS analysis. Fig. 2 shows the S_{2p} spectrum of each surface. An S_{2p} signal at approximately 163 eV was observed on PMPC-*b*-PGMA brushes and PGMA brushes; this signal could be assigned to neutral sulfur species (e.g., disulfide) [42]. On the PMPC-*b*-PGMA brushes, there was a nitrogen peak at approximately 400 eV in addition to that from phosphorylcholine in MPC at about 403 eV (data not shown). We also observed a N_{1s} signal at 400.6 eV on the PGMA brush, which has no nitrogen atom itself. These signals can be attributed to nitrogen in the pyridyl disulfide moieties. As a control, PMPC brushes with no epoxy groups were subjected to the same reaction, and there was no S_{2p} signal. It was

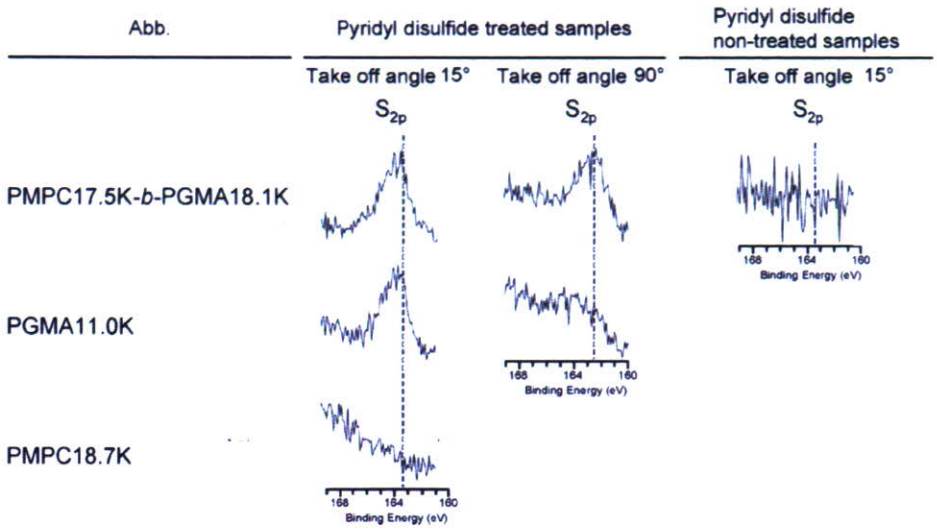

Fig. 2. XPS spectra of polymer brushes treated and not treated with pyridyl disulfide introduction reaction.

also confirmed that no S_{2p} signal was present on the PMPC-*b*-PGMA brushes without the introduction reaction. These results suggest that pyridyl disulfide moieties could be introduced in polymer brushes for reaction via the epoxy groups in the GMA units. Table 2 shows the composition of each surface determined by XPS analysis at a take-off angle of 15°. The sulfur ratio of PMPC14.9K-*b*-PGMA10.1K and PMPC17.5K-*b*-PGMA18.1K was 0.7% and 1.2%, respectively, also confirming that the introduction of pyridyl disulfide moieties could be performed via GMA units.

3.3. Immobilization of Fab' fragments on activated polymer brushes

We immobilized Fab' fragments on polymer brushes by the thiol-disulfide interchange reaction via thiol groups in Fab' fragments and pyridyl disulfide moieties in polymer brushes defining the orientation of the antibodies (Fig. 3). The polymer brushes without pyridyl disulfide moieties were also used as control surfaces to investigate the effect of the moieties on the immobilization of antibody fragments. Fig. 4 shows the XPS spectra of polymer bushes after contact with the Fab' fragments. First, the spectra of the polymer brushes with pyridyl disulfide moieties will be discussed. In the PMPC-*b*-PGMA brush, N_{1s} signals at a binding energy of 399.8 and 402.5 eV were observed. These signals could be attributed to the amine group in the Fab' fragment and the choline group in the MPC unit, respectively. This signal assigned to the amine group in the antibody was also detected in the PGMA brush at 400.0 eV. S_{2p} signals at a binding energy of 163.3 and 163.5 eV were observed in the PMPC-*b*-PGMA brush and the PGMA brush, respectively, indicating the existence of disulfide. In contrast, in the control surfaces without the pyridyl disulfide moieties, nitrogen signals from the antibody fragments were detected but the intensity was lower than that from the surfaces having the pyridyl disulfide moieties. Furthermore, no S_{2p} signal was observed in these non-activated polymer brushes. The experimental atomic ratios were calculated from the atomic percentages and compared between polymer brushes consisting of the same composition. N/Si was 1.6 and 0.4 for the activated PMPC-*b*-PGMA brush and the non-activated PMPC-*b*-PGMA brush, respectively. The ratio of nitrogen from antibody and MPC was also calculated giving 1.4 for the activated PMPC-*b*-PGMA brush and 0.9 for the non-activated PMPC-*b*-PGMA brush. On the PGMA brushes, the activated PGMA brush showed higher a ratio of N/Si (1.1) than did that of the PGMA brush without the pyridyl disulfide moieties (0.4). The relatively large amount of nitrogen in the activated polymer brushes suggests that the Fab' fragments could be preferentially immobilized via a thiol-disulfide interchange reaction. It is thought that Fab' fragments on non-activated polymer brushes were immobilized via nucleophilic reactions involving amine groups of antibody fragments and

Table 2
Surface composition of polymer brushes determined by XPS analysis

Abbreviation	XPS data (take off angle 15) (%)						
	C	O	N	P	Si	Br	S
PMPC14.9K-*b*-PGMA10.1K	60.2	28.6	2.6	2.2	5.8	0.0	0.7
PMPC17.5K-*b*-PGMA18.1K	63.4	29.0	1.4	1.2	3.9	0.0	1.2
PGMA11.0K	64.4	28.2	0.4	0.1	5.8	0.0	1.0
PMPC18.7K	32.2	42.5	0.4	1.4	23.6	0.0	0.0
PMPC17.5K-*b*-PGMA18.1K[a]	67.6	27.8	1.0	1.4	2.2	0.0	0.0

[a] Sample not treated with pyridyl disulfide.

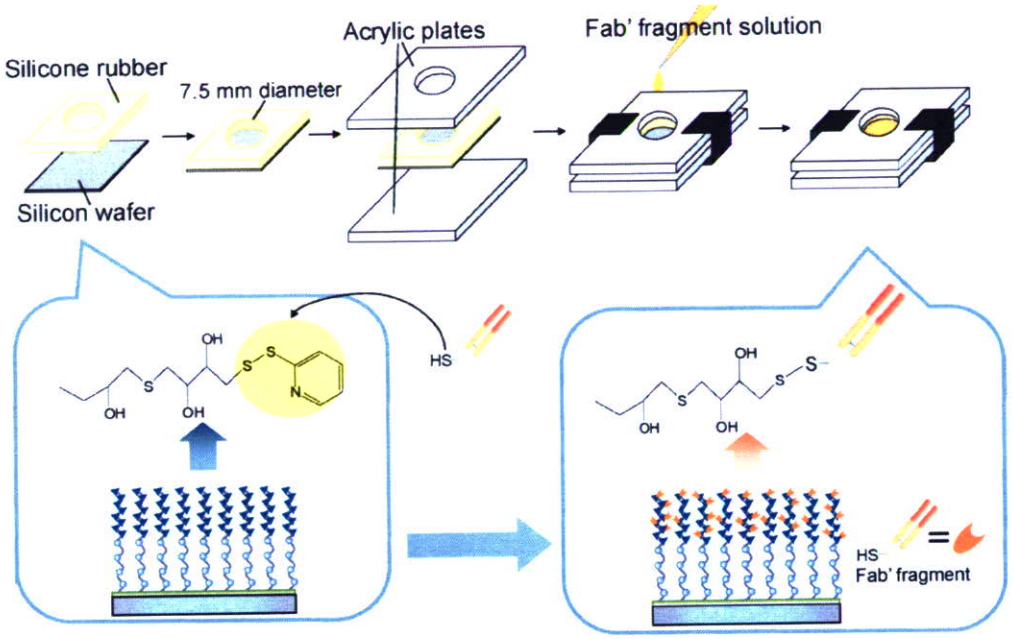

Fig. 3. Scheme of Fab' fragment-immobilization in defined area of surface.

epoxy groups of the polymer brushes in random orientation, or adsorbed nonspecifically. The occurrence of nonspecific adsorption of antibody fragments must be also considered in the case of using activated surfaces. The PMPC brush was also placed in contact with the Fab' fragment solution as a control, and the nitrogen atom from the antibody was not detected, thereby confirming the ability of PMPC to suppress biofouling.

To compare the amount of immobilized antibody, FITC-labeled Fab' fragments were reacted with each surface with pyridyl disulfide moieties and the fluorescence intensity was analyzed. We prepared an organosilane monolayer having epoxy groups (epoxysilane films) as a control surface because it is often used as a substrate for biosensors to immobilize biomolecules such as DNA and protein. Fig. 5 is a comparison of the fluorescence intensity. The amount of immobilized antibody in the PMPC-*b*-PGMA brushes changed with the length of the PGMA unit. PMPC-*b*-PGMA brushes with longer PGMA units and PGMA brushes could immobilize larger amounts of Fab' fragments compared with epoxysilane films, showing 2.3 times and 4.1 times larger fluorescence intensity than that of the epoxysilane films, respectively.

3.4. Reaction with antigen of Fab' fragment-immobilized surfaces

The activity of immobilized antibody fragments was investigated by the reaction with an FITC-labeled antigen (Fig. 6). Fig. 7 shows the ratio of the fluorescence intensity of each surface. The fluorescence intensity of the epoxysilane films was considered as a standard for the ratio. The values of the polymer brushes was higher than that of the epoxysilane films, suggesting that the polymer brush surfaces were effective for

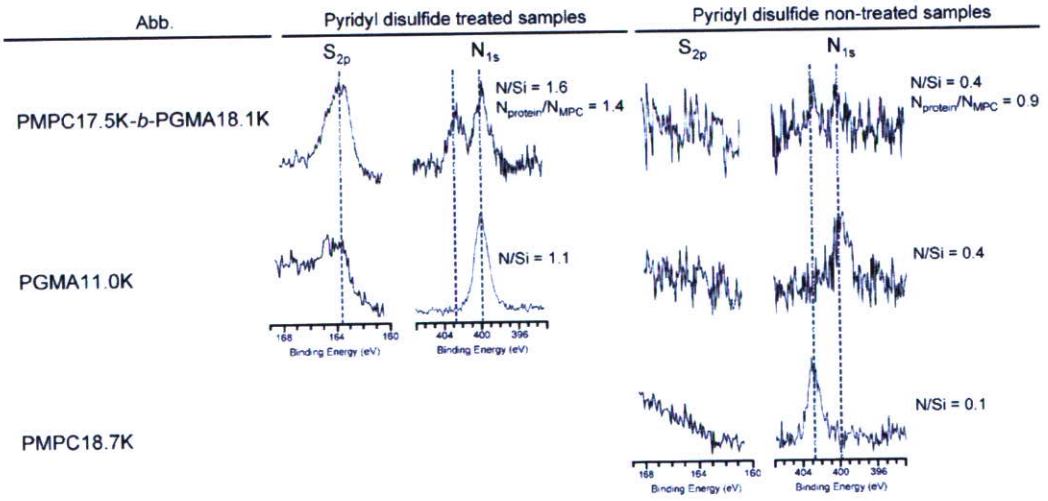

Fig. 4. XPS spectra of polymer brushes treated and not treated with pyridyl disulfide after contact with Fab' fragments.

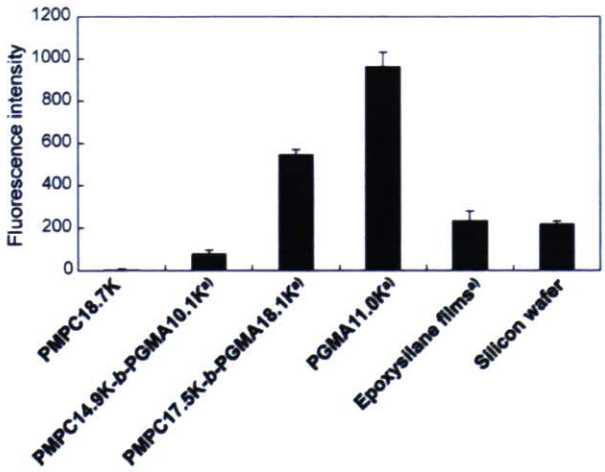

Fig. 5. Fluorescence intensity of each surface after contact with FITC-labeled Fab' fragments. (a) Samples treated with pyridyl disulfide.

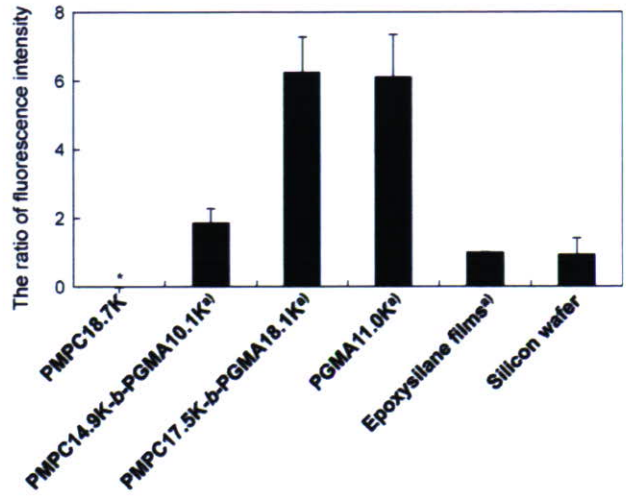

Fig. 7. Ratio of fluorescence intensity of each surface after contact with FITC-labeled antigen (the fluorescence intensity of epoxysilane films was determined as the standard for the ratio). (*) N.D.; (a): samples were treated with pyridyl disulfide and Fab' fragments were immobilized on these surfaces before the reaction with antigen.

reaction with the antigen compared with the epoxysilane films. It was shown that Fab' fragment-immobilized PMPC14.9K-*b*-PGMA10.1K, PMPC17.5K-*b*-PGMA18.1K, and PGMA11.0K had 1.9-, 6.2-, and 6.1-fold higher reactivity with the antigen than did that of epoxysilane films, respectively. In PMPC-*b*-PGMA brushes, the fluorescence intensity increased with an increase in the thickness of the PGMA unit, indicating that we could control the reaction with an antigen by changing the length of the PGMA unit. When we compared Fig. 5 with Fig. 7, it was obvious that antibody fragments on PGMA11.0K and PMPC17.5K-*b*-PGMA18.1K showed similar reactivity with antigens (Fig. 7) although PGMA11.0K immobilized larger amounts of Fab' fragments than did that of PMPC17.5K-*b*-PGMA18.1K (Fig. 5). This result implied that Fab' fragments immobilized on PMPC17.5K-*b*-PGMA18.1K could react with antigens more effectively than that on PGMA11.0K. While the molecular weight of the PGMA unit in PMPC17.5K-*b*-PGMA18.1K is larger than that of PGMA11.0K, PGMA11.0K grafted to a silicon wafer more densely than did a PGMA unit to PMPC17.5K-*b*-PGMA18.1K (Table 1). Then, the number of GMA monomer units in the defined area as N (U/nm^2) was calculated according to the value in Table 1 and the following equation:

$$N = \frac{M_n \sigma}{F_w} \tag{2}$$

where M_n is the theoretical number-average molecular weight of each polymer brush, σ is the graft density of PGMA, and F_w is the molecular weight of the GMA monomer (142.15 g/mol). N of PGMA11.0K and PMPC17.5K-*b*-PGMA18.1K were 33.3 and 33.1, respectively, showing almost the same value for these polymer brushes. This implies that the capacity of immobilizing Fab' fragments is the same in these two kinds of polymer brushes. Therefore, it can be assumed that the difference in the amount of immobilized antibody fragments is due to the differences between the polymer brushes such as the conformation, accessibility by Fab' fragments, and influence of nonspecific adsorption. For the reason of achieving an efficient reaction with the antigens of the antibody fragments immobilized on

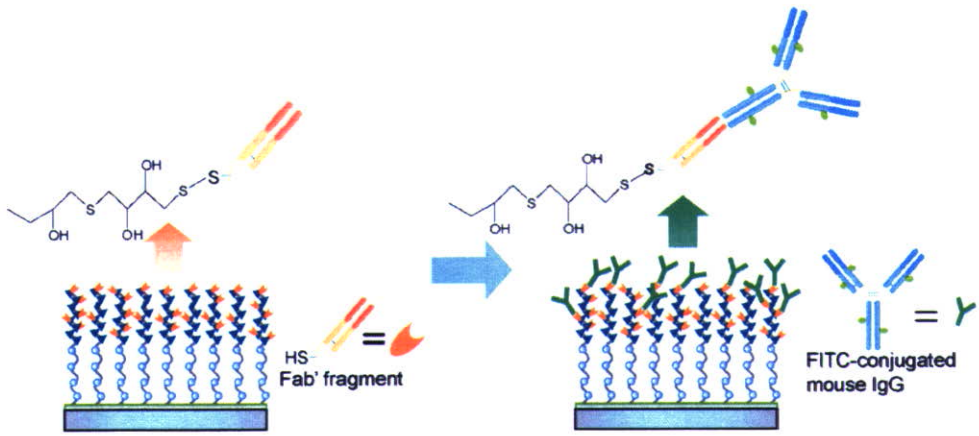

Fig. 6. Reaction with FITC-labeled IgG of immobilized Fab' fragments on polymer brushes.

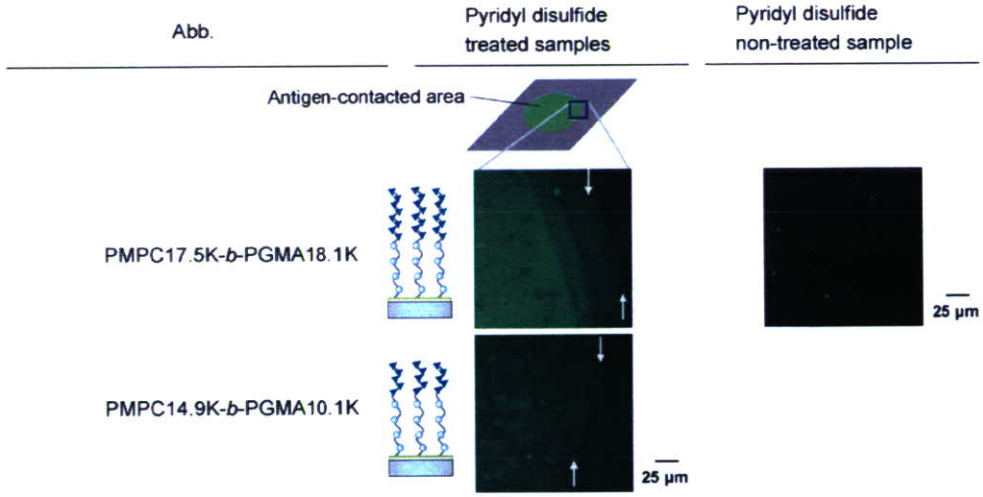

Fig. 8. Pictures observed with a fluorescent microscope of block copolymer brushes after the immobilization of Fab' fragments and the subsequent reaction with antigen.

PMPC17.5K-*b*-PGMA18.1K, it is thought that the condition of the Fab' fragments is different between the PGMA brush and the PMPC-*b*-PGMA brush, which has biocompatible PMPC under PGMA [43]. It was demonstrated that the control of surface chemistry and structure at the molecular level influenced the activity of the immobilized antibody.

The effect of the orientation of the immobilized antibody was also investigated. Polymer brushes without pyridyl disulfide moieties were used for the immobilization of Fab' fragments and subsequent reaction with FITC-labeled antigens in the same experiment with the activated polymer brushes. A fluorescence intensity about 20 times greater was observed on the PMPC-*b*-PGMA brush with the pyridyl disulfide moieties than that on the non-activated PMPC-*b*-PGMA brush (data not shown). Photographs of the observation with the fluorescent microscope are shown in Fig. 8. In the activated polymer brushes, the fluorescence intensity in the Fab' fragment-immobilized and antigen-contacted area was greater than that of the non-contacted area, and the boundary could be observed. In contrast, on the polymer brushes without the pyridyl disulfide moieties, almost no difference between the areas where the antigen was contacted and not contacted was seen. These results demonstrated the effectiveness of oriented immobilization of antibody fragments without affecting the antigen-binding domain.

3.5. Nonspecific protein adsorption on Fab' fragment-immobilized polymer brushes

To reduce nonspecific interactions with biomolecules that are not analytes is crucial for achieving highly sensitive biorecognition. Therefore, the ability to suppress nonspecific adsorption of proteins on antibody fragment-immobilized surfaces was examined. Fab' fragments were immobilized on activated surfaces and subsequently rhodamine-labeled IgG, which is not an antigen of the immobilized antibody fragments was contacted. Fig. 9 compares the fluorescence intensity after contact

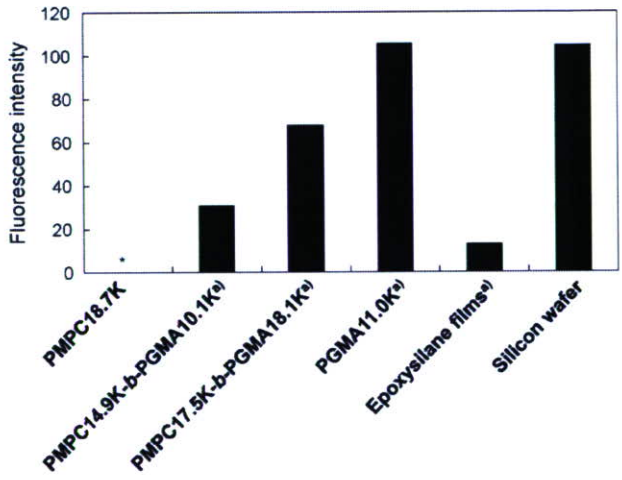

Fig. 9. Fluorescence intensity of each surface after contact with rhodamine-labeled donkey IgG. (*) N.D.; (a): samples were treated with pyridyl disulfide and Fab' fragments were immobilized on these surfaces before the contact with rhodamine-labeled IgG.

with the rhodamine-labeled IgG. A larger amount of protein was adsorbed on the polymer brushes than on the epoxysilane films. The adsorption of IgG was increased with the length of the PGMA unit in the block copolymer brushes, suggesting that IgG was mainly adsorbed on the PGMA unit. Although the number of GMA monomer units in the defined area is the same between PGMA11.0K and PMPC17.5K-*b*-PGMA18.1K as described above, relatively low protein adsorption was observed in PMPC17.5K-*b*-PGMA18.1K compared to that in PGMA11.0K. It is thought that the suppressed adsorption of proteins on PMPC17.5K-*b*-PGMA18.1K is because the PMPC unit has a property to suppress nonspecific adsorption of proteins. This result indicates that further optimization of brush structure to reduce nonspecific protein adsorption is required.

4. Conclusion

In this study, we have demonstrated the oriented immobilization of antibody fragments onto polymer brushes consisting of PMPC and PGMA having epoxy groups that can be used to immobilize biomolecules. Covalent immobilization of antibody fragments in an oriented state on well-defined polymer brushes was performed via a thiol-disulfide interchange reaction. Changing the thickness of the PGMA unit enabled control of the amount of immobilized Fab' fragments and subsequent reaction with antigens. The effectiveness of polymer brushes for reaction with antigens compared to that of the epoxysilane films was shown. In addition, the structural differences of the polymer brushes influenced the biological reactions, showing higher reactivity of antigens with antibody fragments on PMPC-*b*-PGMA brushes having biocompatible PMPC units than that of PGMA brushes. Further investigation of polymer brush structures is needed. However, the characteristics of PMPC and the dense immobilization of antibodies in defined orientation are attractive for developing highly sensitive biorecognition surfaces.

Acknowledgment

The authors of this paper would like to thank the Japan Society for the Promotion of Science for its financial supports (18·628, 18681018) of this research.

References

[1] F. Rusmini, Z. Zhong, J. Feijen, Biomacromolecules 8 (2007) 1775.
[2] P. Angenendt, Drug Discov. Today 10 (2005) 503.
[3] L. Sage, Anal. Chem. 76 (2004) 137A.
[4] S.V. Rao, K.W. Anderson, L.G. Bachas, Mikrochim. Acta 128 (1998) 127.
[5] P. Peluso, D.S. Wilson, D. Do, H. Tran, M. Venkatasubbaiah, D. Quincy, B. Heidecker, K. Poindexter, N. Tolani, M. Phelan, K. Witte, L.S. Jung, P. Wagner, S. Nock, Anal. Biochem. 312 (2003) 113.
[6] S. Chen, L. Liu, J. Zhou, S. Jiang, Langmuir 19 (2003) 2859.
[7] H. Wang, D.G. Castner, B.D. Ratner, S. Jiang, Langmuir 20 (2004) 1877.
[8] Y. Nagasaki, H. Kobayashi, Y. Katsuyama, T. Jomura, T. Sakura, J. Colloid Interface Sci. 309 (2007) 524.
[9] X. Huang, M.J. Wirth, Anal. Chem. 69 (1997) 4577.
[10] X. Huang, M.J. Wirth, Macromolecules 32 (1999) 1694.
[11] M. Ejaz, S. Yamamoto, K. Ohno, Y. Tsujii, T. Fukuda, Macromolecules 31 (1998) 5934.
[12] M. Ejaz, S. Yamamoto, Y. Tsujii, T. Fukuda, Macromolecules 35 (2002) 1412.
[13] Y. Iwasaki, A. Mikami, K. Kurita, N. Yui, K. Ishihara, N. Nakabayashi, J. Biomed. Mater. Res. 36 (1997) 508.
[14] Y. Iwasaki, S. Sawada, N. Nakabayashi, G. Khang, H.B. Lee, K. Ishihara, Biomaterials 20 (1999) 2185.
[15] K. Ishihara, E. Ishikawa, Y. Iwasaki, N. Nakabayashi, J. Biomater. Sci., Polym. Ed. 10 (1999) 1047.
[16] Y. Iwasaki, N. Nakabayashi, K. Ishihara, J. Biomed. Mater. Res. 57 (2001) 72.
[17] K. Ishihara, H. Oshida, Y. Endo, T. Ueda, A. Watanabe, N. Nakabayashi, J. Biomed. Mater. Res. 26 (1992) 1543.
[18] K. Ishihara, H. Nomura, T. Mihara, K. Kurita, Y. Iwasaki, N. Nakabayashi, J. Biomed. Mater. Res. 39 (1998) 323.
[19] Y. Iwasaki, S. Sawada, K. Ishihara, G. Khang, H.B. Lee, Biomaterials 23 (2002) 3897.
[20] S. Sawada, S. Sakaki, Y. Iwasaki, N. Nakabayashi, K. Ishihara, J. Biomed. Mater. Res. 64A (2003) 411.
[21] R. Iwata, P. Suk-In, V.P. Hoven, A. Takahara, K. Akiyoshi, Y. Iwasaki, Biomacromolecules 5 (2004) 2308.
[22] W. Feng, S. Zhu, K. Ishihara, J.L. Brash, Langmuir 21 (2005) 5980.
[23] W. Feng, J.L. Brash, S. Zhu, Biomaterials 27 (2006) 847.
[24] R. Iwata, Y. Iwasaki, K. Akiyoshi, A. Takahara, Trans. Mater. Res. Soc. Jpn. 30 (2005) 735.
[25] F.J. Xu, Q.J. Cai, Y.L. Li, E.T. Kang, K.G. Neoh, Biomacromolecules 6 (2005) 1012.
[26] G. Pirri, M. Chiari, F. Damin, A. Meo, Anal. Chem. 78 (2006) 3118.
[27] Z. Zhang, S. Chen, S. Jiang, Biomacromolecules 7 (2006) 3311.
[28] S. Tugulu, A. Arnold, I. Sielaff, K. Johnsson, H.A. Klok, Biomacromolecules 6 (2005) 1602.
[29] K. Ishihara, T. Ueda, N. Nakabayashi, Polym. J. 22 (1990) 355.
[30] K. Matyjaszewski, P.J. Miller, N. Shukla, B. Immaraporn, A. Gelman, B.B. Luokala, T.M. Siclovan, G. Kickelbick, T. Vallant, H. Hoffmann, T. Pakula, Macromolecules 32 (1999) 8716–8724.
[31] A. Ramakrishnan, R. Dhamodharan, J. Ruhe, Macromol. Rapid Commun. 23 (2002) 612–616.
[32] I. Luzinov, D. Julthongpiput, A. Liebmann-Vinson, T. Cregger, M.D. Foster, V.V. Tsukruk, Langmuir 16 (2000) 504.
[33] R.G.A. Jones, T.-A. Alsop, R. Hull, R. Tierney, P. Rigsby, J. Holley, D. Sesardic, Toxicon 48 (2006) 246.
[34] M. Husemann, E.E. Malmstrom, M. McNamara, M. Mate, D. Mecerreyes, D.G. Benoit, J.L. Hedrick, P. Mansky, E. Huang, T.P. Russell, C.J. Hawker, Macromolecules 32 (1999) 1424–1431.
[35] M. Ejaz, K. Ohno, Y. Tsujii, T. Fukuda, Macromolecules 33 (2000) 2870.
[36] K. Brocklehurst, J. Carlsson, M.P.J. Kierstan, Biochem. J. 133 (1973) 573.
[37] J. Carlsson, R. Axen, T. Unge, Eur. J. Biochem. 59 (1975) 567.
[38] V. Grazu, O. Abian, C. Mateo, F. Batista-Viera, R. Fernandez-Lafuente, J.M. Guisan, Biomacromolecules 4 (2003) 1495.
[39] D.H. Na, B.H. Woo, K.C. Lee, Bioconjugate Chem. 10 (1999) 306.
[40] D. Bontempo, K.L. Heredia, B.A. Fish, H.D. Maynard, J. Am. Chem. Soc. 126 (2004) 15372.
[41] G. Ledung, M. Bergkvist, A.P. Quist, U. Gelius, J. Carlsson, S. Oscarsson, Langmuir 17 (2001) 6056.
[42] T.L. Brower, M. Cook, A. Ulman, J. Phys. Chem. B 107 (2003) 11721.
[43] S. Sakaki, Y. Iwasaki, N. Nakabayashi, K. Ishihara, Polym. J. 32 (2000) 637.